References

1. WHO World malaria report 2012.
2. Murray CJ, Rosenfeld LC, Lim SS, Andrews KG, Foreman KJ, et al. (2012) Global malaria mortality between 1980 and 2010: a systematic analysis. Lancet 379: 413–431.
3. Chauhan VS, Yazdani SS, Gaur D (2010) Malaria vaccine development based on merozoite surface proteins of *Plasmodium falciparum*. Hum Vaccin 6(9): 757–762.
4. Healer J, Murphy V, Hodder AN, Masciantonio R, Gemmill AW, et al. (2004) Allelic polymorphisms in apical membrane antigen-1 are responsible for evasion of antibody-mediated inhibition in *Plasmodium falciparum*. Mol Microbiol 52(1): 159–168.
5. Horii T, Shirai H, Jie L, Ishii KJ, Palacpac NMQ, et al. (2010) Evidences of protection against blood-stage infection of *Plasmodium falciparum* by the novel protein vaccine SE36. Parasitol Int 59(3): 380–386.
6. Palacpac NMQ, Ntege E, Yeka A, Balikagala B, Suzuki N, et al. (2013) Phase 1b randomized trial and follow-up study in Uganda of the blood-stage malaria vaccine candidate BK-SE36. PLoS ONE 8(5), e64073.
7. Palacpac NMQ, Arisue N, Tougan T, Ishii KJ, Horii T (2011) *Plasmodium falciparum* serine repeat antigen 5 (SE36) as a malaria vaccine candidate. Vaccine 29(35): 5837–5845.
8. Li J, Mitamura T, Fox BA, Bzik DJ, Horii T (2002) Differential localization of processed fragments of *Plasmodium falciparum* serine repeat antigen and further processing of its N-terminal 47 kDa fragment. Parasitol Int 51(4): 343–352.
9. Aoki S, Li J, Itagaki S, Okech BA, Egwang TG, et al. (2002) Serine repeat antigen (SERA5) is predominantly expressed among the SERA multigene family of *Plasmodium falciparum*, and the acquired antibody titers correlate with serum inhibition of the parasite growth. J Biol Chem 277(49): 47533–47540.
10. Yeoh S, O'Donnell RA, Koussis K, Dluzewski AR, Ansell KH, et al. (2007) Subcellular discharge of a serine protease mediates release of invasive malaria parasites from host erythrocytes. Cell 131(6): 1072–1083.
11. Tanabe K, Arisue N, Palacpac NM, Yagi M, Tougan T, et al. (2012) Geographic differentiation of polymorphism in the *Plasmodium falciparum* malaria vaccine candidate gene SERA5. Vaccine 30(9): 1583–1593.
12. Okech BA, Nalunkuma A, Okello D, Pang XL, Suzue K, et al. (2001) Natural human immunoglobulin G subclass responses to *Plasmodium falciparum* serine repeat antigen in Uganda. Am J Trop Med Hyg 65(6): 912–917.
13. Okech B, Mujuzi G, Ogwal A, Shirai H, Horii T, et al. (2006) High titers of IgG antibodies against *Plasmodium falciparum* serine repeat antigen 5 (SERA5) are associated with protection against severe malaria in Ugandan children. Am J Trop Med Hyg 74(2): 191–197.
14. Pang XL, Mitamura T, Horii T (1999) Antibodies reactive with the N-terminal domain of *Plasmodium falciparum* serine repeat antigen inhibit cell proliferation by agglutinating merozoites and schizonts. Infect Immun 67(4): 1821–1827.
15. Pang XL, Horii T (1998) Complement-mediated killing of *Plasmodium falciparum* erythrocytic schizont with antibodies to the recombinant serine repeat antigen (SERA). Vaccine 16(13): 1299–1305.
16. Soe S, Singh S, Camus D, Horii T, Druilhe P (2002) *Plasmodium falciparum* serine repeat protein, a new target of monocyte-dependent antibody-mediated parasite killing. Infect Immun 70(12): 7182–7184.
17. Fox BA, Pang XL, Suzue K, Horii T, Bzik DJ (1997) *Plasmodium falciparum*: an epitope within a highly conserved region of the 47-kDa amino-terminal domain of the serine repeat antigen is a target of parasite-inhibitory antibodies. Exp Parasitol 85(2): 121–134.
18. Fox BA, Horii T, Bzik DJ (2002) *Plasmodium falciparum*: fine-mapping of an epitope of the serine repeat antigen that is a target of parasite-inhibitory antibodies. Exp Parasitol 101(1): 69–72.
19. Uversky VN (2011) Intrinsically disordered proteins from A to Z. Int J Biochem Cell Biol 43(8): 1090–1103.
20. Tompa P (2012) Intrinsically disordered proteins: a 10-year recap. Trends Biochem Sci 37(12): 509–516.
21. Zilversmit MM, Volkman SK, DePristo MA, Wirth DF, Awadalla P, et al. (2010) Low-complexity regions in *Plasmodium falciparum*: missing links in the evolution of an extreme genome. Mol Biol Evol 27(9): 2198–2209.
22. Mohan A, Sullivan WJ Jr, Radivojac P, Dunker AK, Uversky VN (2008) Intrinsic disorder in pathogenic and non-pathogenic microbes: discovering and analyzing the unfoldomes of early-branching eukaryotes. Mol Biosyst 4(4): 328–340.
23. Zhang X, Perugini MA, Yao S, Adda CG, Murphy VJ, et al. (2008) Solution conformation, backbone dynamics and lipid interactions of the intrinsically unstructured malaria surface protein MSP2. J Mol Biol 379(1): 105–121.
24. Olugbile S, Kulangara C, Bang G, Bertholet S, Suzarte E, et al. (2009) Vaccine potentials of an intrinsically unstructured fragment derived from the blood stage-associated *Plasmodium falciparum* protein PFF0165c. Infect Immun 77(12): 5701–5709.
25. Kulangara C, Luedin S, Dietz O, Rusch S, Frank G, et al. (2012) Cell biological characterization of the malaria vaccine candidate trophozoite exported protein 1. PLoS One. 7(10): e46112.
26. Bueno LL, Lobo FP, Morais CG, Mourão LC, de Ávila RA, et al. (2011) Identification of a highly antigenic linear B cell epitope within *Plasmodium vivax* apical membrane antigen 1 (AMA-1). PLoS One. 6(6): e21289.
27. Bouharoun-Tayoun H, Attanath P, Sabchareon A, Chongsuphajaisiddhi T, Druilhe P (1990) Antibodies that protect humans against *Plasmodium falciparum* blood stages do not on their own inhibit parasite growth and invasion in vitro, but act in cooperation with monocytes. J Exp Med 172(6): 1633–1641.
28. Jafarshad A, Dziegiel MH, Lundquist R, Nielsen LK, Singh S, et al. (2007) A novel antibody-dependent cellular cytotoxicity mechanism involved in defense against malaria requires costimulation of monocytes FcγRII and FcγRIII. J Immunol 178(5): 3099–3106.
29. Druilhe P, Spertini F, Soesoe D, Corradin G, Mejia P, et al. (2005) A malaria vaccine that elicits in humans antibodies able to kill *Plasmodium falciparum*. PLoS Med 2(11): e344.
30. Kim OTP, Yura K, Go N (2006) Amino acid residue doublet propensity in the protein-RNA interface and its application to RNA interface prediction. Nucleic Acids Res 34(22): 6450–6460.
31. Emanuelsson O, Brunak S, von Heijne G, Nielsen H (2007) Locating proteins in the cell using TargetP, SignalP, and related tools. Nat Protoc 2(4): 953–971.
32. Thompson JD, Higgins DG, Gibson TJ (1994) CLUSTAL W: improving the sensitivity of progressive multiple sequence alignment through sequence weighting, position-specific gap penalties and weight matrix choice. Nucleic Acids Res 22(22): 4673–4680.
33. Combet C, Blanchet C, Geourjon C, Deléage G (2000) NPS@: network protein sequence analysis. Trends Biochem Sci 25(3): 147–150.
34. Igarashi Y, Heureux E, Doctor KS, Talwar P, Gramatikova S, et al. (2009) PMAP: databases for analyzing proteolytic events and pathways. Nucleic Acids Res 37:D611–618.
35. Gill SC, von Hippel PH (1989) Calculation of protein extinction coefficients from amino acid sequence data. Anal Biochem 182(2): 319–326.
36. Sabchareon A, Burnouf T, Ouattara D, Attanath P, Bouharoun-Tayoun H, et al. (1991) Parasitologic and clinical human response to immunoglobulin administration in *falciparum* malaria. Am J Trop Med Hyg 45(3): 297–308.
37. Bouharoun-Tayoun H, Oeuvray C, Lunel F, Druilhe P (1995) Mechanisms underlying the monocyte-mediated antibody-dependent killing of *Plasmodium falciparum* asexual blood stages. J Exp Med 182(2): 409–418.
38. Liu J, Perumal NB, Oldfield CJ, Su EW, Uversky VN, et al. (2006) Intrinsic disorder in transcription factors. Biochemistry 45(22): 6873–6888.
39. Hilser VJ, Thompson EB (2011) Structural dynamics, intrinsic disorder, and allostery in nuclear receptors as transcription factors. J Biol Chem 286(46): 39675–39682.
40. Shoemaker BA, Portman JJ, Wolynes PG (2000) Speeding molecular recognition by using the folding funnel: the fly-casting mechanism. Proc Natl Acad Sci U S A 97(16): 8868–8873.
41. Levy Y, Onuchic JN, Wolynes PG (2007) Fly-casting in protein-DNA binding: frustration between protein folding and electrostatics facilitates target recognition. J Am Chem Soc 129(4): 738–739.
42. Adda CG, MacRaild CA, Reiling L, Wycherley K, Boyle MJ, et al. (2012) Antigenic characterization of an intrinsically unstructured protein, *Plasmodium falciparum* merozoite surface protein 2. Infect Immun 80(12): 4177–4185.
43. Pan W, Huang D, Zhang Q, Qu L, Zhang D, et al. (2004) Fusion of two malaria vaccine candidate antigens enhances product yield, immunogenicity, and antibody-mediated inhibition of parasite growth *in vitro*. J Immunol 172(10): 6167–6174.

Vaccine 32 (2014) 3004–3009

Contents lists available at ScienceDirect

Vaccine

journal homepage: www.elsevier.com/locate/vaccine

Hemozoin is a potent adjuvant for hemagglutinin split vaccine without pyrogenicity in ferrets

Motoyasu Onishi[a,b,c], Mitsutaka Kitano[a], Keiichi Taniguchi[a], Tomoyuki Homma[a], Masanori Kobayashi[a], Akihiko Sato[a], Cevayir Coban[d], Ken J. Ishii[b,c,*]

[a] Infectious Diseases, Medicinal Research Laboratories, Shionogi & Co., Ltd., Osaka, Japan
[b] Laboratory of Adjuvant Innovation, National Institute of Biomedical Innovation (NIBIO), Osaka, Japan
[c] Laboratory of Vaccine Science, Immunology Frontier Research Center (IFREC), World Premier Institute (WPI), Osaka University, Osaka, Japan
[d] Laboratory of Malaria Immunology, Immunology Frontier Research Center (IFREC), World Premier Institute (WPI), Osaka University, Osaka, Japan

ARTICLE INFO

Article history:
Received 21 November 2013
Received in revised form 14 February 2014
Accepted 25 March 2014
Available online 8 April 2014

Keywords:
Vaccine
Adjuvant
Influenza
Fluad
Ferret
Seasonal trivalent HA split vaccine

ABSTRACT

Background: Synthetic hemozoin (sHZ, also known as β-hematin) from monomeric heme is a particle adjuvant which activates antigen-presenting cells (APCs), such as dendritic cells and macrophages, and enhances humoral immune responses to several antigens, including ovalbumin, human serum albumin, and serine repeat antigen 36 of *Plasmodium falciparum*. In the present study, we evaluated the adjuvanticity and pyrogenicity of sHZ as an adjuvant for seasonal trivalent hemagglutinin split vaccine (SV) for humans using the experimental ferret model.
Method: Ferrets were twice immunized with trivalent SV, SV with sHZ (SV/sHZ) or Fluad, composed of trivalent SV with MF59. Serum hemagglutination inhibition (HI) titers against three viral hemagglutinin (HA) antigens were measured at every week after the immunization. The pyrogenicity of SV/sHZ was examined by monitoring the body temperature of the immunized ferrets. To evaluate the protective efficacy of SV/sHZ, the immunized ferrets were challenged with influenza virus B infection, followed by measurement of viral titers in the nasal cavity and body temperature.
Results: sHZ enhanced HI titers against three viral HA antigens in a dose-dependent manner, to an extent comparable to that of Fluad. The highest dose of sHZ (800 μg) immunized with SV conferred sterile protection against infection with heterologous Influenza B virus, without causing any pyrogenic reaction such as high fever.
Conclusion: In the present study, sHZ enhanced the protective efficacy of SV against influenza infection without inducing pyrogenic reaction, suggesting sHZ to be a promising adjuvant candidate for human SV.

© 2014 The Authors. Published by Elsevier Ltd. This is an open access article under the CC BY-NC-SA license (http://creativecommons.org/licenses/by-nc-sa/3.0/).

1. Introduction

Hemozoin (HZ) is a detoxification product of heme molecules persisting in the food vacuoles of *Plasmodium* parasite [1,2]. Purified HZ activates innate immune responses via Toll-like receptor (TLR)9 in antigen-presenting cells (APCs), including myeloid and plasmacytoid dendritic cells [3], and enhances humoral responses depending TLR9 but not NACHT, LRR and PYD domains containing the protein 3 (NALP3) inflammasome signaling pathway [4]. Synthetic hemozoin (sHZ, also known as β-hematin) from monomeric heme also activates APCs, and enhances the humoral responses of several antigens, including ovalbumin, human serum albumin, and serine repeat antigen 36 of *Plasmodium falciparum* in mice or cynomolgus monkeys (*Macaca fascicularis*) [4,5]. Moreover, sHZ acts as a potent immune modulator, which suppresses IgE production against house dust allergens, suggesting that sHZ itself might be usable for an allergy vaccine for dogs [4]. Differently from the purified HZ, sHZ enhance the adaptive immune response through MyD88, not related to TLR9 or NALP3 inflammasome pathway [4]. Thus, the efficacy, safety, and immunological mechanisms of sHZ has been demonstrated, further studies are needed to explore its application as an adjuvant for vaccines.

In general, the efficacy of influenza hemagglutinin split vaccine (SV) correlates with the level of neutralizing antibody to

Abbreviations: sHZ, synthetic hemozoin; HA, hemagglutinin; HI, hemagglutination inhibition; SV, hemagglutinin split vaccine; SV/sHZ, hemagglutinin split vaccine adjuvanted with synthetic hemozoin; $TCID_{50}$, 50% tissue culture infective dose.

* Corresponding author at: NIBIO, 7-6-8 Asagi, Saito, Ibaraki, Osaka 5670085, Japan. Tel.: +81 72 641 8043; fax: +81 72 641 8079.
E-mail addresses: kenishii@biken.osaka-u.ac.jp, kenishii@nibio.go.jp (K.J. Ishii).

http://dx.doi.org/10.1016/j.vaccine.2014.03.072
0264-410X/© 2014 The Authors. Published by Elsevier Ltd. This is an open access article under the CC BY-NC-SA license (http://creativecommons.org/licenses/by-nc-sa/3.0/).

hemagglutinin (HA) [6]. The neutralizing antibody contributes to both prevention of influenza infection and suppression of influenza exacerbation. Some reports have estimated the efficacy of influenza vaccine in young adults to be 70–90%, and that in the elderly to be considerably lower, in the range of 17–53% [7]. Hence, SV is required to improve the efficacy for the elderly. One possible solution of the issue is via the use of adjuvant [8], although some adjuvants have been reported to cause pyrogenic reaction associated with the induction of proinflammatory cytokine responses in clinical studies [9,10]. Therefore, it is important to evaluate the pyrogenicity of adjuvant in clinical or non-clinical studies to enable wider use of adjuvants.

In the present study, we evaluated the efficacy and pyrogenicity of sHZ as an adjuvant for seasonal trivalent SV in the ferret model.

2. Materials and methods

2.1. Antigens and adjuvants

Seasonal influenza SV "BIKEN", containing influenza virus HA surface antigens from three virus strains, A/California/7/2009 (H1N1), A/Victoria/210/2009 (H3N2), and B/Brisbane/60/2008, was obtained from The Research Foundation for Microbial Diseases of Osaka University (Osaka, Japan) [11]. Endotoxin-free sHZ chemically synthesized using an acidic method was obtained from Invivogen (San Diego, CA) [12]. The particle size of sHZ was determined by SEM and found to be approximately 1–2 μm. Fluad, composed of influenza virus HA surface antigens from the three strains described above and MF59, was obtained from Novartis Vaccines and Diagnostics, Inc. (Emeryville, CA) [13].

2.2. Virus and cells

Influenza virus B/Osaka/32/2009 was kindly provided by Osaka Prefectural Institute of Public Health. Madin–Darby canine kidney (MDCK) cells were obtained from the American Type Culture Collection (Manassas, VA) and were grown in minimum essential medium (MEM; Invitrogen, Carlsbad, CA) supplemented with 10% fetal bovine serum (Invitrogen) and 100 μg/ml kanamycin sulfate (Invitrogen) in a humidified atmosphere of 5% CO_2 at 37 °C.

2.3. Ferrets

Approximately 7- to 8-month-old female ferrets were purchased from Marshall Bioresources Japan Inc. (Ibaragi, Japan) and Japan SLC Inc. (Shizuoka, Japan). The experiments were performed under applicable laws and guidelines and after approval from the Shionogi Animal Care and Use Committee. Under anesthesia, at least 1 week before virus inoculation, a data logger (DS1921H-F5; Maxim Integrated Products, Inc., Sunnyvale, CA) was subcutaneously implanted into each ferret to monitor body temperature as previously reported [14]. The absence of influenza A/California/7/2009 (H1N1), A/Victoria/210/2009 (H3N2), and B/Brisbane/60/2008 virus-specific antibody in serum from each ferret was confirmed by hemagglutination inhibition (HI) test before the first immunization.

2.4. HI assay

HI assay was performed according to the protocol previously reported [14]. Serum was treated with receptor-destroying enzyme (RDEII; Denka Seiken, Tokyo, Japan). Serially diluted sera were mixed with 4 HA units of virus antigen for 1 h at room temperature. The mixture was then incubated with 0.5% chicken red blood cells for 30 min at room temperature. The HI titers were expressed as reciprocals of the highest dilution of serum samples that completely inhibited hemagglutination.

2.5. Immunization and sample collection

Ferrets were subcutaneously immunized with 22.5 μg of SV, 22.5 μg of SV adjuvanted with 50–800 μg of sHZ (SV/sHZ (50–800 μg)) or premix solution Fluad, which is composed of 22.5 μg of SV and MF59. Second immunizations were conducted 28 days after the first immunization. Serum was collected by vena cava puncture on the day of the first immunization and 7, 14, 21, 28, and 35 days after the first immunization, and HI titers against three HA antigens, A/California/7/2009 (H1N1), A/Victoria/210/2009 (H3N2), and B/Brisbane/60/2008, were determined.

2.6. Evaluation of pyrogenicity of vaccine with adjuvant in ferrets

Ferrets were subcutaneously immunized with saline or 22.5 μg of SV adjuvanted with 800 μg of sHZ. Body temperatures were monitored every 15 min with the data logger implanted in the ferrets.

2.7. Evaluation of protective effect of vaccine against influenza virus infection

Under anesthesia, ferrets were inoculated intranasally with B/Osaka/32/2009 (1.0×10^4 $TCID_{50}$) in 400 μl of phosphate-buffered saline (PBS). To monitor virus replication in nasal cavities, nasal washes were collected from infected ferrets on days 1 to 6 after infection. The collected samples were stored at below −80 °C until use. For virus titration, serial dilutions of nasal washes were inoculated onto confluent MDCK cells in 96-well plates. After 1 h incubation, the suspension was removed, and the cells were cultured in MEM including 0.5% bovine serum albumin (BSA; Sigma-Aldrich) and 3 μg/ml trypsin. The plates were incubated at 37 °C in 5% CO_2 for 3 days. The presence of cytopathic effects (CPEs) was determined under a microscope, and viral titers were calculated as $\log_{10}$ of $TCID_{50}$/ml. When no CPE was observed using undiluted viral solution, it was defined as an undetectable level, which was considered to be lower than 1.4 $\log_{10}$ of $TCID_{50}$/ml.

2.8. Activation of the inflammasome in peritoneal resident macrophages

Activation of the inflammasome in peritoneal resident macrophages was examined according to the protocol previously reported [15]. Briefly, peritoneal resident macrophages were collected from C57BL/6 mice (Charles River Laboratories Japan, Inc., Kanagawa, Japan) and were prepared with complete RPMI1640 medium (Invitrogen). Macrophages were primed with 50 ng/ml LPS (Sigma-Aldrich) for 18 h and then stimulated with sHZ or Alum (Invivogen) for 8 h. The concentration of IL-1β in supernatant was measured by ELISA (R&D systems, Minneapolis, MN).

2.9. Statistical analysis

Viral titers and body temperature of each animal were calculated as the area under the curve (AUC) by the trapezoidal method. Statistical significance between groups was determined by Dunnett's multiple comparison test using the statistical analysis software SAS (version 9.2) for Windows (SAS Institute, Cary, NC).

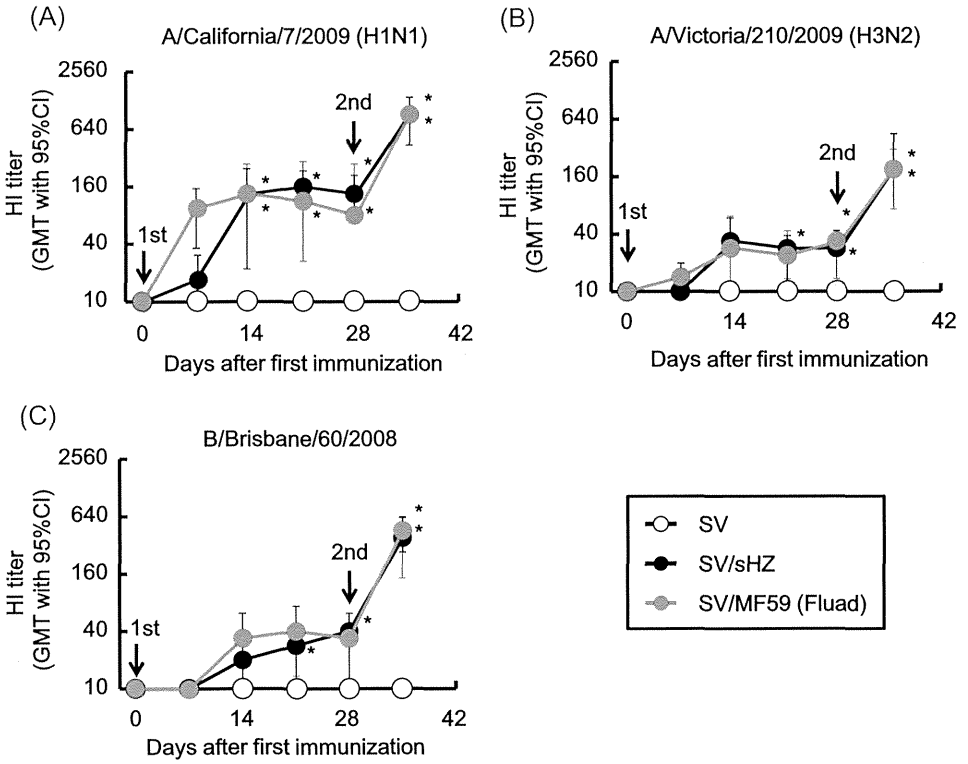

Fig. 1. Evaluation of the immunogenicity of SV, SV/sHZ, and Fluad. Ferrets were twice immunized with SV, SV/sHZ (800 μg) or Fluad. Serum were collected on day 0, 7, 14, 21, 28, and 35 after the first immunization, and HI titers against three HA antigens of A/California/7/2009(H1N1) (A), A/Victoria/210/2009 (H3N2) (B), and B/Brisbane/60/2008 (C) were measured. * $p < 0.05$ by Dunnett's multiple comparison test vs. SV group ($n = 4$ per group). Data represent the GMT ± 95% confidence interval.

3. Results

3.1. sHZ enhanced immunogenicity of HA split vaccine in a dose-dependent manner

To examine the adjuvant effect of sHZ on HA split vaccine, ferrets ($n = 4$ per group) were twice immunized with SV with or without sHZ (800 μg) or Fluad, and then their serum HI titers were measured every week. Fluad is composed of SV adjuvanted with MF59, a licensed squalene-based emulsion, widely used in clinical settings [16]. On day 28 after the first immunization, HI titers of SV/sHZ group against H1, H3, and B virus antigens were significantly up-regulated, of which the GMT was 135, 28, and 40, respectively, comparable to those elicited by MF59 ($p < 0.05$, Fig. 1A–C). After the second immunization, HI titers of the SV/sHZ group against all three antigens were significantly higher than those of the SV group on day 35 ($p < 0.05$) (Fig. 1A–C). The GMTs of the HI titers against H1, H3, and B antigens in the SV/sHZ group were 905, 190, and 381, respectively. The boosting effect of sHZ was also comparable to that of MF59. By contrast, HI titers against three HA antigens of the SV group were not enhanced at every analysis point (Fig. 1A–C). These results demonstrated that sHZ has a potent adjuvanticity to enhance the immunogenicity of SV, and its activity was comparable to that of MF59 in ferrets.

Next, the dose-dependent adjuvanticity of sHZ to enhance the immunogenicity of SV was examined. Ferrets were twice immunized with SV/sHZ (50–800 μg), and HI titers were measured at every week. The adjuvanticity to enhance HI titers against HA antigens of H1 and B was observed with at least 200 μg of sHZ after the first immunization, but no boosting effect of 200 μg of sHZ was observed after the second immunization (Fig. 2). Overall, each HI titer against all three HA antigens of SV/sHZ (800 μg) was 3–20 fold higher than that of SV/sHZ (200 μg) on day 7 after the second immunization. Thus, 800 μg of sHZ showed higher adjuvanticity than 200 μg of sHZ. This result implied that sHZ enhanced the immunogenicity of SV in a dose-dependent manner in ferrets.

3.2. HA split vaccine adjuvanted with sHZ did not cause pyrogenic reaction after immunization

It is reported that the ferret model can evaluate not only the efficacy of vaccine but also the pyrogenicity of immunostimulatory agents like TLR ligands (e.g. TLR7/8 agonist R848) and virion components, and non-pyrogenicity of SV [17,18] To evaluate the pyrogenicity of sHZ after the first immunization, ferrets were immunized with saline or SV/sHZ (800 μg), and the body temperatures of ferrets were monitored continuously. The results showed that sHZ did not enhance the body temperature after immunization, and no difference was observed in body temperature between the SV/sHZ and the saline groups, suggesting that sHZ does not have the potential to induce a pyrogenic reaction in ferrets (Fig. 3).

3.3. sHZ enhanced the protective efficacy of HA split vaccine against influenza virus infection

Having observed such potent adjuvanticity without pyrogenicity of sHZ in ferrets, we next evaluated the contribution of sHZ-adjuvanted SV vaccine to its protective efficacy. On day 7 after the second immunization, the ferrets were intranasally infected with B/Osaka/32/2009, and viral titers in nasal cavities were measured daily after infection. On day 2 after infection, each viral titer of two groups SV/sHZ (200 μg) and SV/sHZ (800 μg) was significantly lower than that of the SV group ($p < 0.01$ and <0.001, respectively) (Fig. 4A). Each viral titer AUC of SV/sHZ (200 μg and 800 μg) groups was significantly lower than that of the SV group ($p < 0.01$) (Fig. 4C).

The body temperature changes of ferrets were monitored from 2 days before to 5 days after infection. Comparing the SV group with the SV/sHZ group showed that the elevations of body temperature

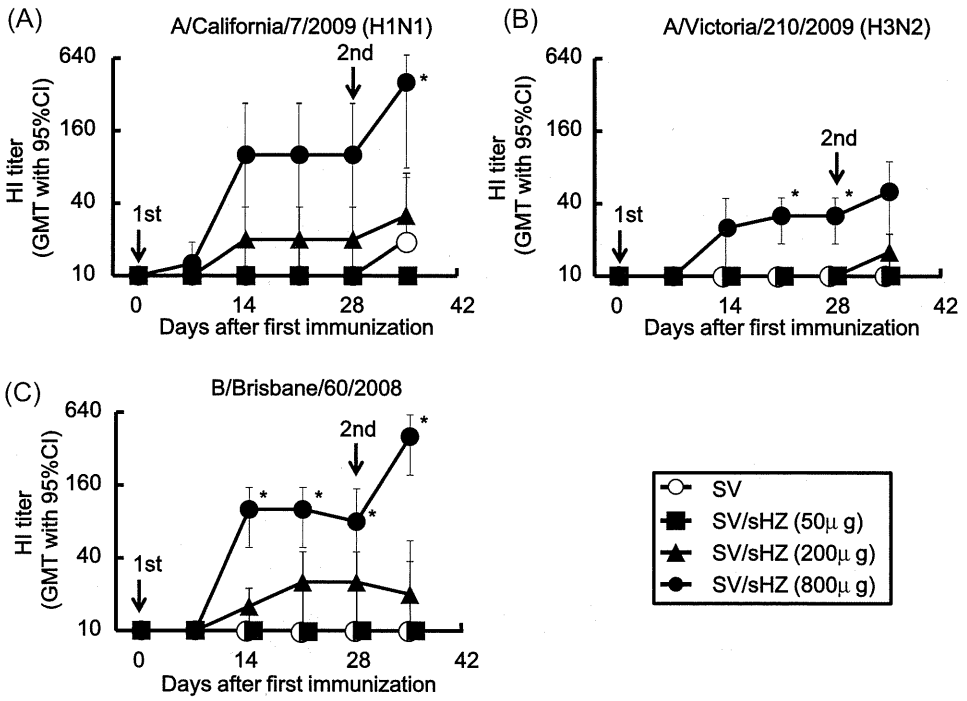

Fig. 2. Evaluation of the dose responses of sHZ to enhance HI antibody responses against three HA antigens. Ferrets were twice immunized with SV ($n=6$) or SV/sHZ (50, 200 or 800 μg) ($n=3$). Serum were collected on day 0, 7, 14, 21, 28, and 35 after the first immunization, and HI titers against three HA antigens of A/California/7/2009(H1N1) (A), A/Victoria/210/2009 (H3N2) (B), and B/Brisbane/60/2008 (C) were measured. * $p<0.05$ by Dunnett's multiple comparison test vs. SV group. Data represent the GMT ± 95% confidence interval.

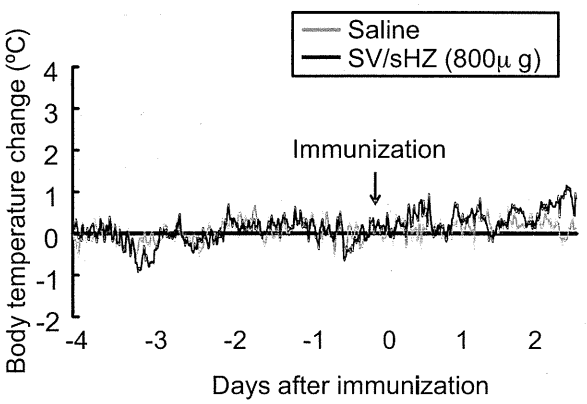

Fig. 3. Evaluation of pyrogenicity of SV/sHZ. Ferrets were immunized with saline or SV/sHZ (800 μg) ($n=2$–3). Body temperatures of ferrets were recorded every 15 min by a data logger which had been implanted subcutaneously. The data were plotted from the average of body temperature changes every 15 min. Gray and black lines indicate the saline and the SV/sHZ groups, respectively. Baseline was set as the average of body temperature during the 2 days before immunization.

were suppressed in all SV/sHZ groups in a dose-dependent manner (Fig. 4B). Moreover, body temperature change AUCs of all SV/sHZ groups were lower than that of the SV vaccine group (Fig. 4D).

4. Discussion

Vaccination is the primary strategy to prevent influenza infection [19]. The efficacy of influenza vaccine in young and healthy adults is estimated to be 70–90%, but that in the elderly is lower at 17–53% [7]. Dose escalation of antigen has been examined to enhance the efficacy of vaccine for the elderly [20]. However, this is not a realistic approach without improvement of the manufacturing plants or manufacturing systems. As an alternative strategy, the use of adjuvant may help overcome these issues by enhancing the immunogenicity of influenza vaccine. In the present study, sHZ enhanced the immunogenicity of SV and consequently elevated its protective efficacy against virus infection in the ferret model, which has been shown to reflect influenza symptoms and protective immune responses to influenza infection in humans [21]. In particular, SV/sHZ (800 μg) strongly suppressed the viral titer below the detection limit and did not cause pyrogenic reaction after immunization. These results suggested sHZ to be a promising adjuvant candidate for human SV.

Pyrogenicity is one of the main issues in the development of novel adjuvants for vaccine even with good adjuvanticity. Therefore, minimizing toxicity remains one of the major challenges in adjuvant research [22]. Treanor et al. reported that VAX125, a recombinant HA influenza-flagellin fusion vaccine, showed high immunogenicity in clinical study [23], but in some cases, febrile symptoms were observed in the first 24 h following vaccination. It was suggested that the pyrogenic reaction was associated with systemic proinflammatory cytokine responses. sHZ induces the production of IL-1β by activating NALP3 inflammasome pathway in macrophages [24,25]. However, in the present study, sHZ did not cause pyrogenic reaction after the first immunization. To find insights into why sHZ did not show pyrogenicity, the activity of sHZ to induce the NALP3 inflammasome was examined, and the results revealed that a relatively high concentration (≥300 μg/ml) of sHZ was required to induce IL-1β production in macrophages (Supplemental Fig. 1). Dostert et al. also demonstrated that 150 μg/ml sHZ could induce inflammasome in bone marrow-derived macrophages [25]. These results suggested that the activation of NALP3-inflammasome caused by sHZ was very low and did not act as a trigger to cause a pyrogenic reaction in ferrets.

Rapid systemic distribution of adjuvant is also understood to enhance the risk of causing a pyrogenic reaction. Sauder et al. reported that R848, which is known as an imidazoquinoline compound and TLR7/8 agonist, caused a pyrogenic reaction correlated

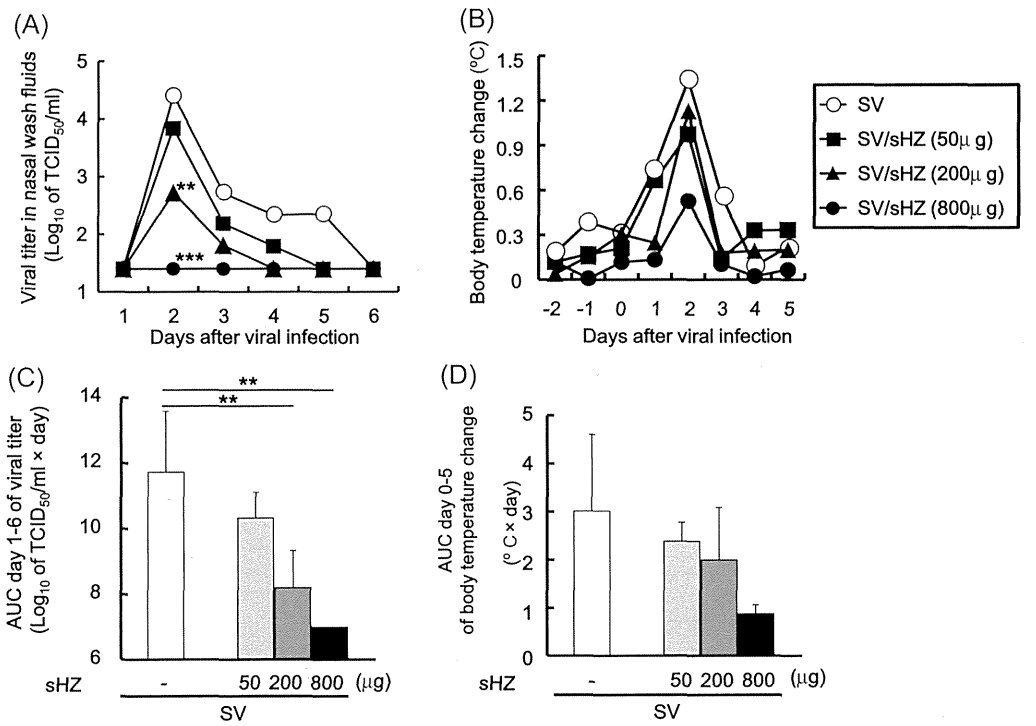

Fig. 4. Evaluation of the protective efficacy of SV/sHZ against virus infection. B/Osaka/32/2009 (1.0×10^4 $TCID_{50}$) was intranasally infected to ferrets immunized with SV ($n=6$) or SV/sHZ (50, 200 or 800 μg) ($n=3$). Nasal wash fluids were collected on days 1–6 after infection, and viral titers were measured (A). Data represent the means. Viral titer AUCs were calculated using the trapezoidal rule on the basis of means of the viral titers ($TCID_{50}$/ml) on days 1 to 6 (C). Data represent the mean ± standard deviation. Body temperatures of ferrets were recorded every 60 min by data logger which had been subcutaneously implanted. The baseline of the body temperature was set as the average of body temperature during the 2 days before infection. The data were plotted from the average of body temperature changes during 1 day (B). Data represent the mean. Body temperature change AUCs were calculated by use of the trapezoidal rule on the basis of the means of the body temperature change on days 0 to 5 (D). Data represent the mean ± standard deviation. ** $p<0.01$, *** $p<0.001$ by Dunnett's multiple comparison test vs. SV group.

with the induction of proinflammatory cytokine responses in healthy adults [10]. This strong response was caused by rapid systemic distribution of R848 after administration [10]. 3M-052 is a lipid-modified imidazoquinoline compound derived from R848, bearing a C18 lipid moiety, for sustained release and incorporation into a bilayer liposome [26]. 3M-052 incorporated into liposome composed of dioleoylphosphatidylcholine (3M-052/PC) was shown to avoid the induction of systemic proinflammatory cytokine responses [26]. In addition, the adjuvanticity of 3M-052/PC was higher than that of R848. Therefore, persistent immunostimulation at the injected site with adjuvant is thought to contribute to its potent adjuvanticity [26]. sHZ, synthesized by an acidic method, formed insoluble particles approximately 1–2 μm in size. On day 35 after the first immunization, a small amount of sHZ was observed at the immunized site (data not shown), suggesting that the distribution of sHZ was not rapid or was very limited in ferrets. Thus, slow systemic distribution of sHZ might contribute to prevent a pyrogenic reaction and maintain potent adjuvanticity after immunization. The size of particle adjuvant is considered to affect the particulate-induced immune responses such as the efficient activation of dendritic cells or adjuvant uptake of macrophages [27]. The smaller particles (20–200 nm) are usually uptaken by endocytosis via clathrin-coated vesicles, caveolae or their independent receptors, and preferentially ingested by dendritic cells. The larger size particles (0.5–5 μm) are uptaken by macropinocytosis, while particles greater than 0.5 μm are predominantly taken up by phagocytosis, and primarily ingested by macrophages [28]. The crystal size of sHZ can be adjusted by the modification of synthetic method, and smaller size sHZ (diameter range; 50 nm–1 μm, peak of the frequency distribution; 50–200 nm) exhibits higher adjuvanticity than larger size sHZ (>5 μm) in mice when immunized with ovalbumin antigen [4]. This size-dependent adjuvanticity of sHZ is considered as the result from the manner of uptake of APCs. In this study, we demonstrated the potent adjuvanticity of sHZ, which contains approximately 1–2 μm particles.

In the present study, we demonstrated that sHZ could enhance the protective efficacy of SV against influenza virus in ferrets without causing a pyrogenic reaction. The findings of this study indicate that sHZ is safe and has great potential for use as an adjuvant for human SV.

Funding sources

This study was financially supported by Shionogi & Co., Ltd. a contrated collaboration between NIBIO and Shionogi & Co., Ltd.

Author contributions

M.O., M. Kitano, K.T., T.H., M. Kobayashi, A.S., and K.J.I. designed research; M.O., M. Kitano, K.T., T.H., and M. Kobayashi performed research; M.O., M. Kitano, and K.T. analyzed data; M.O. drafted the article; T.H., C.C. and K.J.I. revised the article critically for important intellectual content.

Conflict of interest statement

CC and KJI hold a patent related to synthetic hemozoin. The other authors declare no conflict of interest.

Acknowledgments

We thank Tetsuo Kase from the Osaka Prefectural Institute of Public Health for providing B/Osaka/32/2009 and Makoto Kodama

from Shionogi & Co., Ltd. for help with the animal care and experiments.

Appendix A. Supplementary data

Supplementary material related to this article can be found, in the online version, at http://dx.doi.org/10.1016/j.vaccine.2014.03.072.

References

[1] Sullivan DJ. Theories on malarial pigment formation and quinoline action. Int J Parasitol 2002;32(13):1645–53.
[2] Arese P, Schwarzer E. Malarial pigment (haemozoin): a very active 'inert' substance. Ann Trop Med Parasitol 1997;91(5):501–16.
[3] Coban C, Ishii KJ, Kawai T, Hemmi H, Sato S, Uematsu S, et al. Toll-like receptor 9 mediates innate immune activation by the malaria pigment hemozoin. J Exp Med 2005;201(1):19–25.
[4] Coban C, Igari Y, Yagi M, Reimer T, Koyama S, Aoshi T, et al. Immunogenicity of whole-parasite vaccines against *Plasmodium falciparum* involves malarial hemozoin and host TLR9. Cell Host Microbe 2010;7(1):50–61.
[5] Tougan T, Aoshi T, Coban C, Katakai Y, Kai C, Yasutomi Y, et al. TLR9 adjuvants enhance immunogenicity and protective efficacy of the SE36/AHG malaria vaccine in nonhuman primate models. Hum Vaccines Immunother 2013;9(2):283–90.
[6] Cox RJ, Brokstad KA, Ogra P. Influenza virus: immunity and vaccination strategies. Comparison of the immune response to inactivated and live, attenuated influenza vaccines. Scand J Immunol 2004;59(1):1–15.
[7] Goodwin K, Viboud C, Simonsen L. Antibody response to influenza vaccination in the elderly: a quantitative review. Vaccine 2006;24(8):1159–69.
[8] Tetsutani K, Ishii KJ. Adjuvants in influenza vaccines. Vaccine 2012;30(52):7658–61.
[9] Batista-Duharte A, Lindblad EB, Oviedo-Orta E. Progress in understanding adjuvant immunotoxicity mechanisms. Toxicol Lett 2011;203(2):97–105.
[10] Sauder DN, Smith MH, Senta-McMillian T, Soria I, Meng TC. Randomized, single-blind, placebo-controlled study of topical application of the immune response modulator resiquimod in healthy adults. Antimicrob Agents Chemother 2003;47(12):3846–52.
[11] Tanimoto T, Nakatsu R, Fuke I, Ishikawa T, Ishibashi M, Yamanishi K, et al. Estimation of the neuraminidase content of influenza viruses and split-product vaccines by immunochromatography. Vaccine 2005;23(37):4598–609.
[12] Coban C, Yagi M, Ohata K, Igari Y, Tsukui T, Horii T, et al. The malarial metabolite hemozoin and its potential use as a vaccine adjuvant. Allergol Int 2010;59(2):115–24.
[13] Puig Barbera J, Gonzalez Vidal D. MF59-adjuvanted subunit influenza vaccine: an improved interpandemic influenza vaccine for vulnerable populations. Expert Rev Vaccines 2007;6(5):659–65.
[14] Kitano M, Itoh Y, Kodama M, Ishigaki H, Nakayama M, Ishida H, et al. Efficacy of single intravenous injection of peramivir against influenza B virus infection in ferrets and cynomolgus macaques. Antimicrob Agents Chemother 2011;55(11):4961–70.
[15] Kuroda E, Ishii KJ, Uematsu S, Ohata K, Coban C, Akira S, et al. Silica crystals and aluminum salts regulate the production of prostaglandin in macrophages via NALP3 inflammasome-independent mechanisms. Immunity 2011;34(4):514–26.
[16] Della Cioppa G, Nicolay U, Lindert K, Leroux-Roels G, Clement F, Castellino F, et al. Superior immunogenicity of seasonal influenza vaccines containing full dose of MF59 ((R)) adjuvant: results from a dose-finding clinical trial in older adults. Hum Vaccines Immunother 2012;8(2):216–27.
[17] Kitano M, Homma T, Taniguchi K, Oonishi M, Kobayashi M, Sato A, et al. Pyrogenicity evaluation of influenza vaccine with TLR agonists in ferret. In: Sixth Vaccine & ISV Annual Global Congress. 2012.
[18] Pickering JM, Smith H, Sweet C. Influenza virus pyrogenicity: central role of structural orientation of virion components and involvement of viral lipid and glycoproteins. J Gen Virol 1992;73(Pt 6):1345–54.
[19] Lambert LC, Fauci AS. Influenza vaccines for the future. N Engl J Med 2010;363(21):2036–44.
[20] Couch RB, Winokur P, Brady R, Belshe R, Chen WH, Cate TR, et al. Safety and immunogenicity of a high dosage trivalent influenza vaccine among elderly subjects. Vaccine 2007;25(44):7656–63.
[21] Matsuoka Y, Lamirande EW, Subbarao K. The ferret model for influenza. Curr Protoc Microbiol 2009:2 (Chapter 15:Unit 15G).
[22] Aguilar JC, Rodriguez EG. Vaccine adjuvants revisited. Vaccine 2007;25(19):3752–62.
[23] Treanor JJ, Taylor DN, Tussey L, Hay C, Nolan C, Fitzgerald T, et al. Safety and immunogenicity of a recombinant hemagglutinin influenza-flagellin fusion vaccine (VAX125) in healthy young adults. Vaccine 2010;28(52):8268–74.
[24] Shio MT, Eisenbarth SC, Savaria M, Vinet AF, Bellemare MJ, Harder KW, et al. Malarial hemozoin activates the NLRP3 inflammasome through Lyn and Syk kinases. PLoS Pathog 2009;5(8):e1000559.
[25] Dostert C, Guarda G, Romero JF, Menu P, Gross O, Tardivel A, et al. Malarial hemozoin is a Nalp3 inflammasome activating danger signal. PLoS One 2009;4(8):e6510.
[26] Smirnov D, Schmidt JJ, Capecchi JT, Wightman PD. Vaccine adjuvant activity of 3M-052: an imidazoquinoline designed for local activity without systemic cytokine induction. Vaccine 2011;29(33):5434–42.
[27] Kuroda E, Coban C, Ishii K. Particulate adjuvant and innate immunity: past achievements, present findings, and future prospects. Int Rev Immunol 2013;32(2):209–20.
[28] Xiang SD, Scholzen A, Minigo G, David C, Apostolopoulos V, Mottram PL, et al. Pathogen recognition and development of particulate vaccines: does size matter? Methods 2006;40(1):1–9.

nature COMMUNICATIONS

ARTICLE

Received 24 Sep 2013 | Accepted 4 Mar 2014 | Published 10 Apr 2014

DOI: 10.1038/ncomms4566

Nucleic acid sensing by T cells initiates Th2 cell differentiation

Takayuki Imanishi[1], Chitose Ishihara[1], Mohamed El Sherif Gadelhaq Badr[1], Akiko Hashimoto-Tane[1], Yayoi Kimura[2], Taro Kawai[3,†], Osamu Takeuchi[3,†], Ken J. Ishii[4,5], Shun'ichiro Taniguchi[6], Tetsuo Noda[7], Hisashi Hirano[2], Frank Brombacher[8], Glen N. Barber[9], Shizuo Akira[3] & Takashi Saito[1,10]

While T-cell responses are directly modulated by Toll-like receptor (TLR) ligands, the mechanism and physiological function of nucleic acids (NAs)-mediated T cell costimulation remains unclear. Here we show that unlike in innate cells, T-cell costimulation is induced even by non-CpG DNA and by self-DNA, which is released from dead cells and complexes with antimicrobial peptides or histones. Such NA complexes are internalized by T cells and induce costimulatory responses independently of known NA sensors, including TLRs, RIG-I-like receptors (RLRs), inflammasomes and STING-dependent cytosolic DNA sensors. Such NA-mediated costimulation crucially induces Th2 differentiation by suppressing T-bet expression, followed by the induction of GATA-3 and Th2 cytokines. These findings unveil the function of NA sensing by T cells to trigger and amplify allergic inflammation.

[1] Laboratory for Cell Signaling, RCAI, RIKEN Center for Integrative Medical Sciences (IMS-RCAI), Yokohama, Kanagawa 230-0045, Japan. [2] Graduate School of Medical Life Sciences, Yokohama City University, Yokohama, Kanagawa 236-0004, Japan. [3] Laboratory of Host Defense, WPI Immunology Frontier Research Center, Osaka University, Suita, Osaka 565-0871, Japan. [4] Laboratory of Adjuvant Innovation, National Institute of Biomedical Innovation, Ibaraki, Osaka 567-0085, Japan. [5] Laboratories of Vaccine Science, WPI Immunology Frontier Research, Osaka University, Suita, Osaka 565-0871, Japan. [6] Department of Molecular Oncology, Institute of Pathogenesis and Disease Prevention, Shinshu University Graduate School of Medicine, Matsumoto, Nagano 390-8621, Japan. [7] Department of Cell Biology, Cancer Research Institute of the Japanese Foundation of Cancer Research, Toshima-ku, Tokyo 170-8455, Japan. [8] International Center for Genetic Engineering and Biotechnology, Cape Town Component and Institute of Infectious Diseases and Molecular Medicine, Faculty of Health Science, Division of Immunology, University of Cape Town, Cape Town, South Africa. [9] Department of Cell Biology and the Sylvester Comprehensive Cancer Center, University of Miami Miller School of Medicine, Miami, Florida 33136, USA. [10] Laboratory for Cell Signaling, WPI Immunology Frontier Research Center, Osaka University, Suita, Osaka 565-0871, Japan. † Present addresses: Laboratory of Molecular Immunobiology, Graduate School of Biological Sciences, Nara Institute of Science and Technology (NAIST), Ikoma, Nara 630-0192, Japan (T.K.); Laboratory of Infection and Prevention, Institute for Virus Research, Kyoto University, Sakyo-ku, Kyoto 606-8507, Japan (O.T.). Correspondence and requests for materials should be addressed to T.S. (email: saito@rcai.riken.jp).

© 2014 Macmillan Publishers Limited. All rights reserved.

Toll-like receptors (TLRs) sense pathogen-associated molecular patterns to initiate not only innate responses but also to help regulate T cell-mediated adaptive immune responses[1,2]. While some TLRs are expressed on the cell surface, NA-sensing TLRs such as TLR3, TLR7/8 and TLR9 are expressed in endosomal compartments, allowing specific recognition of endocytosed pathogens.

Recent studies have shown that T cells also express TLRs and that TLR ligands can directly modulate T-cell responses. For example, TLR2 ligands directly promote proliferation of activated T cells[3,4], modulate the proliferation and suppressive functions of $CD4^+CD25^+$ regulatory T cells[5,6], trigger Th1 effector functions independently of TCR stimulation[7] and modulate Th17 responses[8].

In addition, it has been reported that ligands for NA-sensing TLRs enhance IL-2 production and proliferation of anti-CD3 antibody (Ab)-stimulated T cells[9,10] and promote survival of activated T cells[11], and further that the TLR8 ligand inhibits the suppressive function of regulatory T cells[12]. However, except for TLR2, very little is known about the molecular basis of the NA-sensing mechanisms and the functional consequences of NA-mediated costimulation in T cells.

Naive $CD4^+$ T cells differentiate into various effector T helper (Th) cells such as Th1, Th2 and Th17 cells, which produce IFN-γ, IL-4/IL-5/IL-9/IL-13 and IL-17/IL-22, respectively[13]. While Th1 and Th17 cells exhibit protective functions against intracellular pathogens and extracellular bacteria/fungi, Th2 cells protect from helminthic infection. Contrary to these protective functions, the same Th subsets can play a role in disease pathogenesis: Th1 for inflammatory diseases, Th2 for allergic diseases and Th17 for autoimmune diseases. While TLR stimulation of antigen-presenting cells (APCs) results in the production of IL-12, which induces Th1 differentiation, Th2 development is induced by IL-4, but the cells responsible for the initial wave of IL-4 production needed to induce Th2 differentiation remain elusive[14].

In this study, we report that NA-induced costimulatory responses of $CD4^+$ T cells are mediated independently of known NA sensors in innate immunity. We found that T cells take up NAs to induce costimulation and that the NA-mediated costimulation requires higher-order structure of the NAs by forming complexes with the antimicrobial peptides or with core histones. More importantly, costimulation of naive $CD4^+$ T cell with NAs induces Th2 differentiation through the downregulation of T-bet and the upregulation of GATA-3 expression. Thus, NAs directly induce T-cell costimulation through a unique NA-sensing mechanism to trigger the initial IL-4 production for Th2 differentiation, which might be involved in triggering and amplification of allergic inflammation.

Results

TLR-independent NA-mediated costimulation of $CD4^+$ T cells. To elucidate the functional significance of NA stimulation, naive $CD4^+$ T cells were stimulated with each TLR ligand. While none of the TLR ligands alone were able to induce cell proliferation or IL-2 production, proliferation and IL-2 production were selectively enhanced by Pam3 (TLR1/2), MALP-2 (TLR2/6), poly(I:C) (TLR3) and CpG-B (TLR9) with anti-CD3 stimulation (Fig. 1a).

We next determined whether this response is mediated by TLRs using mice deficient in both MyD88 and TRIF, which lack the capacity to respond to any of the known TLR ligands. Surprisingly, both poly(I:C) and CpG-B-mediated costimulation were normal in the MyD88/TRIF-doubly deficient $CD4^+$ T cells, whereas MALP-2 (TLR2)-mediated costimulation was completely abrogated (Fig. 1b), demonstrating that poly(I:C) and CpG-B-mediated T-cell costimulation was induced independently of TLR signaling.

Notably, DNA lacking CpG motifs required for TLR9 activation, such as non-CpG oligodeoxynucleotide (ODN) and DNA encoding GFP (GFP-S and GFP-AS, antisense strand) could also induce costimulation for IL-2 production (Fig. 1c). These data indicate that DNA induces T-cell costimulation independently of the CpG motifs. We also found that poly(dA), poly(dC) and poly(dG) but not poly(dT) induced the costimulation for IL-2 production, although the uptake of poly(dT) and non-CpG ODN by T cells was comparable (Fig. 1d).

Confocal microscopy analysis revealed that non-CpG ODN colocalized with an endosomal marker dextran and a lysosomal marker LysoTracker (Fig. 1e), indicating that non-CpG ODN is taken up by T cells and transported to endosomes/lysosomes, similarly in innate cells, and induces costimulatory signals in a TLR-independent manner.

Higher-order structure of NA induces T-cell costimulation. It is noteworthy that CpG-A possessing a poly(dG)-tail induced stronger costimulation of $CD4^+$ T cells than other ODNs such as CpG-B and non-CpG (Fig. 1c). The importance of the poly(dG) tract was confirmed by the finding that control ODN GpC corresponding to CpG-A induces robust IL-2 production, similar to CpG-A (Fig. 2a), and that replacement of the poly(dG) motif of GpC by poly(dA), poly(dC) or poly(dT) resulted in the complete loss of stimulatory activity (Fig. 2b).

It has been reported that the poly(dG) tail induces the spontaneous formation of large multimeric aggregates via G-quadruplex formation[15]. Indeed, when GpC was rendered single-stranded by heating and flash-cooling, a dramatic reduction of IL-2 production was observed (Fig. 2c), suggesting that higher-order structures mediated by the poly(dG) motif are critical for enhanced costimulation by CpG-A and GpC. Consistently, introduction of a poly(dG)-tail to non-CpG and CpG-B that possess a phosphodiester (PO) backbone sensitive to DNase enabled them to induce costimulation, whereas the same DNA without the poly(dG)-tail could not (Fig. 2d).

It has been shown that the poly(dG) motif not only protects against DNase degradation[16] but also enhances the cellular uptake of the ODN[17]. Indeed, the uptake of GpC-poly(dC) by T cells was lower than GpC, indicating that GpC-poly(dC) could not induce costimulation due to its poor uptake (Fig. 2e). It is noteworthy that cellular uptake of GpC-poly(dC) was weaker than that of non-CpG (Fig. 2e). It has been reported that phosphorothioate (PS)-modified ODN are taken up more efficiently than PO-ODN[17]. The entire backbone of non-CpG is PS, whereas it is only partial in GpC (Supplementary Table 1). PS modification of GpC-poly(dC) led to enhanced cellular uptake and costimulation (Fig. 2e). By contrast, modification of non-CpG to contain only partial PS resulted in decreased uptake and the failure of costimulation (Fig. 2e). We also confirmed that cellular uptake and costimulation of PO-backboned non-CpG was much weaker than those of PS-backboned non-CpG (Supplementary Fig. 1a). These data indicate that efficient uptake of DNA via its poly(dG) tail or PS modification is critical for induction of costimulation.

While inosine or guanine-containing RNA such as poly(I), poly(G), poly(I:C) and poly(C:G) could induce costimulation, poly(A), poly(U), poly(C) and poly(A:U) could not (Fig. 2f). The induction of costimulation by RNA was correlated with the cellular uptake of RNA (Fig. 2f). These data indicate that RNA-mediated costimulation depends on the RNA sequence for cellular uptake of RNA to induce costimulation.

© 2014 Macmillan Publishers Limited. All rights reserved.

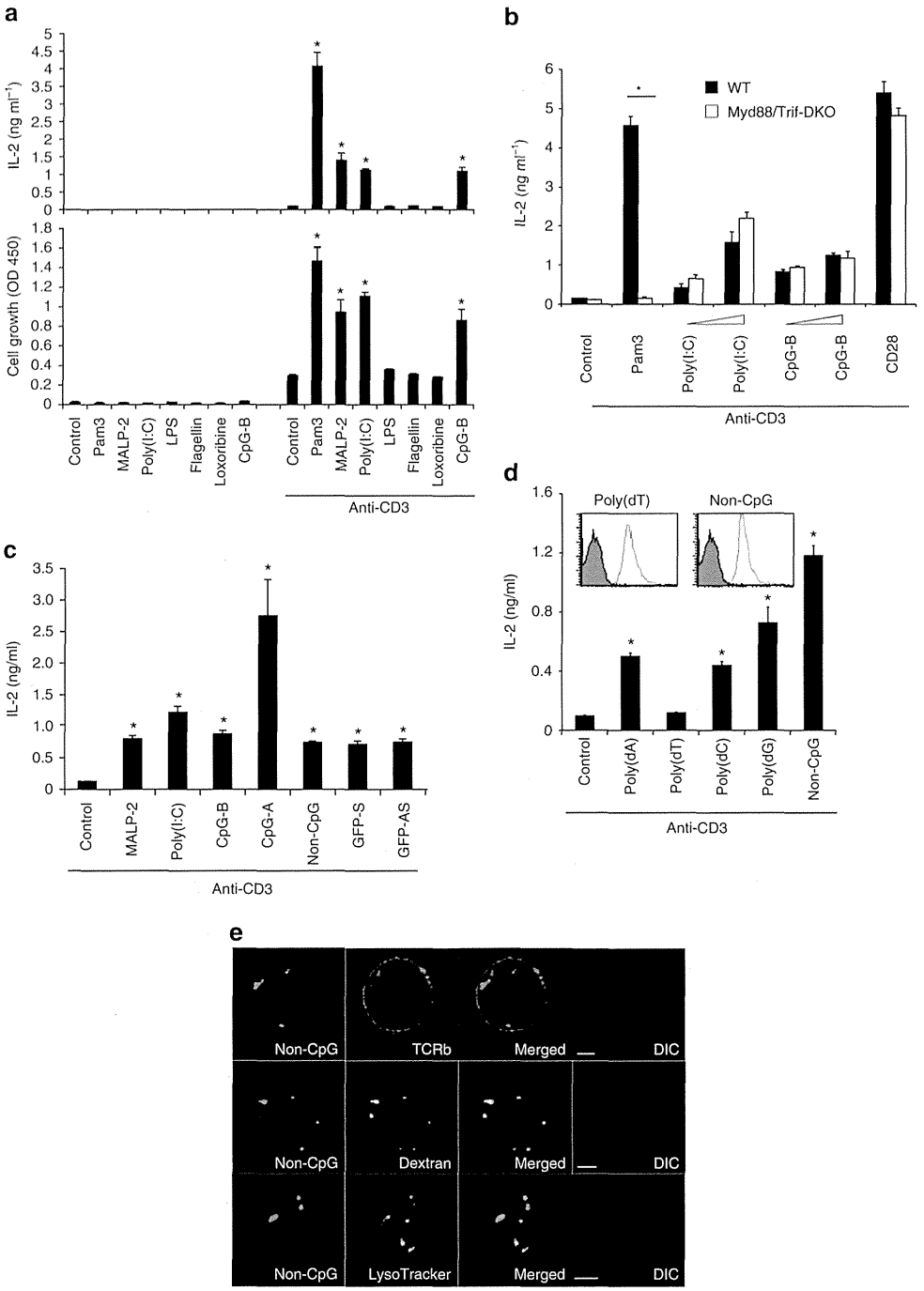

Figure 1 | DNA/RNAs are incorporated into and induce costimulation of CD4$^+$ T cells. (**a**) Naive CD4$^+$ T cells were cultured with indicated TLR ligands (Pam3: 5 μg ml^{-1}, MALP-2: 5 μg ml^{-1}, poly(I:C): 100 μg ml^{-1}, Flagellin: 1 μg ml^{-1}, Loxoribine: 100 μM, CpG-B: 5 μM) in the presence or absence of immobilized anti-CD3ε Ab (10 μg ml^{-1}). After 48-hour incubation, IL-2 production and cell growth were assessed by ELISA and MTS assay, respectively. *$P<0.05$, Student's *t*-test (compared with anti-CD3 alone). (**b**) Naive CD4$^+$ T cells from WT or *Myd88*$^{-/-}$*Trif*$^{-/-}$ mice were stimulated with the indicated TLR ligands or anti-CD28 (Clone: 37.51, 5 μg ml^{-1}) in the presence of immobilized anti-CD3ε Ab. *$P<0.05$, Student's *t*-test (compared with WT cells treated with Pam3). (**c**,**d**) Naive CD4$^+$ T cells were stimulated with the indicated NAs (**c**) and ODNs (**d**) in the presence of immobilized anti-CD3ε Ab. These T cells were incubated with the Cy5-labelled ODNs at 37 °C for 90 min and ODN uptake was determined by flow cytometry (**d**, upper). *$P<0.05$, Student's *t*-test (compared with anti-CD3 alone). (**e**) Naive CD4$^+$ T cells were incubated with 5 μM non-CpG-Cy5 for 90 min and dextran-Alexa Fluor 488 or LysoTracker for last 10 min for the subcellular staining of endosomes and lysosomes, respectively. Confocal microscopy data with differential interference contrast (DIC) images of representative cells are shown. Scale bars, 2.5 μm. Error bars indicate s.d. Data are representative of at least three independent experiments.

It has been reported that poly(I) forms parallel four-stranded helices held together by hydrogen-bonded inosine quartets, similar to poly(dG) chains[18]. We found that heat denaturation of poly(I:C) and poly(G) resulted in impaired costimulation (Fig. 2g), indicating that the ability of RNA to induce T-cell costimulation is dependent on the higher-order structure similar to DNA.

© 2014 Macmillan Publishers Limited. All rights reserved.

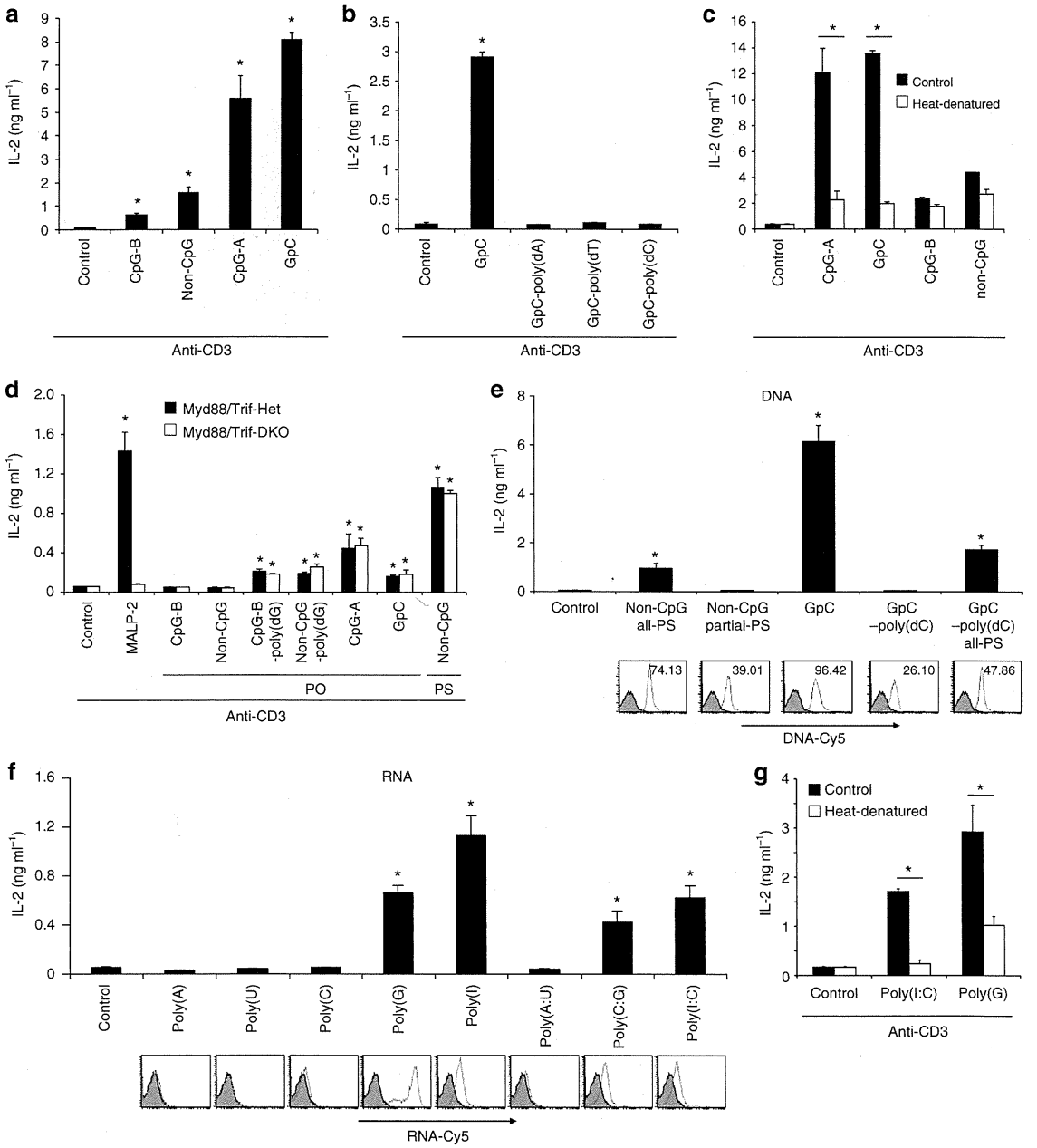

Figure 2 | Properties of DNA/RNAs required for T cell costimulatory activity. (**a**–**c**) Naive CD4$^+$ T cells were activated with plate-bound anti-CD3ε with various DNAs—*$P<0.05$, Student's *t*-test (compared with anti-CD3 alone) (**a**); GpC with different poly tails. *$P<0.05$, Student's *t*-test (compared with anti-CD3 alone) (**b**); and heat-denatured ODNs. *$P<0.01$, Student's *t*-test (compared with the untreated control) (**c**). After 48 h, IL-2 production was measured by ELISA. (**d**) Naive CD4$^+$ T cells derived from *Myd88*$^{+/-}$ *Trif*$^{+/-}$ and *Myd88*$^{-/-}$ *Trif*$^{-/-}$ mice were activated with immobilized anti-CD3ε together with the indicated DNAs. *$P<0.05$, Student's *t*-test (compared with anti-CD3 alone in WT cells). (**e**) Naive CD4$^+$ T cells were stimulated with immobilized anti-CD3ε together with all (all-PS) or partially (partial-PS) PS-modified ODN. CD4$^+$ T cells were incubated with the Cy5-labelled ODN at 37 °C for 90 min, washed and analysed for incorporated ODN by flow cytometry (bottom panels). *$P<0.05$, Student's *t*-test (compared with anti-CD3 alone). (**f**) Naive CD4$^+$ T cells were stimulated with indicated ODNs and analysed similarly as in (**e**). *$P<0.05$, Student's *t*-test (compared with anti-CD3 alone). (**g**) Naive CD4$^+$ T cells were stimulated and analysed similarly in (**c**). *$P<0.05$, Student's *t*-test (compared with the untreated control). Error bars indicate s.d. Data are representative of at least three independent experiments.

Costimulation induced by NA complexed with LL37 and histones. It has been recently shown that endogenous self-DNAs stimulate plasmacytoid dendritic cells by forming aggregated structures upon binding with the antimicrobial peptide LL37 (ref. 19). Similarly, we found that mammalian and bacterial genomic DNA were taken up by T cells and induced costimulation when mixed with LL37 while they alone were neither incorporated nor induce stimulation (Supplementary Fig. 2a, Fig. 3a). Similarly, although poly(A) and poly(A:U) *per se* were defective in cellular uptake and induction of costimulation of naive CD4$^+$ T cells (Fig. 2f), they were incorporated and induced T-cell costimulation when complexed with LL37 (Supplementary Fig. 2b, Fig. 3b).

Similar to LL37, extracellular histones as components of neutrophil extracellular traps exhibit antimicrobial function[20]. We found that the addition of core histones (H2A, H2B, H3 and

© 2014 Macmillan Publishers Limited. All rights reserved.

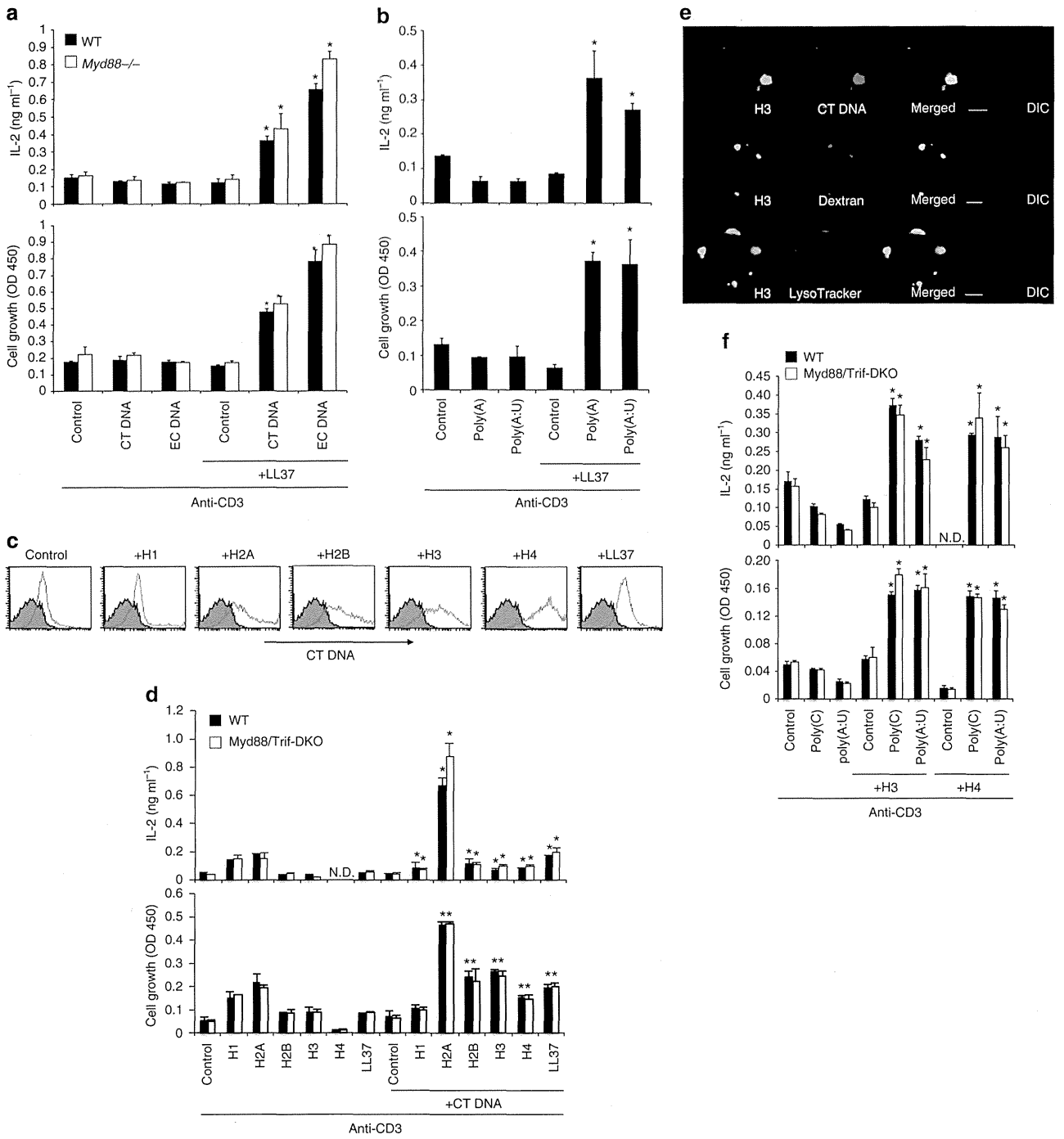

Figure 3 | T-cell activation by NAs complexed with antimicrobial peptides or core histones. (**a**,**b**) Naive CD4$^+$ T cells derived from WT and *Myd88*$^{-/-}$ mice were stimulated with plate-bound anti-CD3ε together with calf thymus (CT)- or *E. coli* (EC)-derived genomic DNA (**a**) or RNAs (**b**) either alone or premixed with LL37. After 48 h, IL-2 production and cell growth were assessed by ELISA and MTS assay, respectively. *$P<0.05$, Student's *t*-test (compared with anti-CD3 plus LL37 in WT cells). (**c**) Naive CD4$^+$ T cells were incubated with the Cy5-labelled CT DNA premixed with the indicated histones or LL37 at 37 °C for 90 min and the incorporated DNA were analysed by flow cytometry. (**d**,**f**) Naive CD4$^+$ T cells derived from WT and *Myd88*$^{-/-}$ *Trif*$^{-/-}$ mice were stimulated with plate-bound anti-CD3 together with CT DNA alone (**d**), RNAs alone (**f**) or premixed with various histones (**d**,**f**), and analysed similarly in (**a**). *$P<0.05$, Student's *t*-test (compared with anti-CD3 plus each histone or LL37 in WT cells). (**e**) Naive CD4$^+$ T cells were stimulated with anti-CD3 with Cy5-labelled CT DNA premixed with Alexa488-labelled histone H3 for 18 h. Endosomes and Lysosomes were visualized by staining with dextran-Alexa Fluor 488 and LysoTracker, respectively. Confocal and differential interference contrast (DIC) images of representative cells are shown. Scale bars, 2.5 μm. Error bars indicate s.d. Data are representative of at least two independent experiments.

H4), but not the linker histone H1, increase cellular uptake of genomic DNA into CD4$^+$ T cells (Fig. 3c). The uptake was correlated with induction of costimulation (Fig. 3d). Although the genomic DNA–H2A complex was the strongest inducer for IL-2 production, H2A itself induces costimulation in the absence of DNA through unknown mechanism. Therefore, we use H3 that has no costimulatory activity by itself to determine the localization of histone/DNA complexes. The genomic

© 2014 Macmillan Publishers Limited. All rights reserved.

DNA–histone H3 complex was incorporated and localized in endosomes and lysosomes as shown by colocalization with dextran and LysoTracker, respectively (Fig. 3e). Similarly to LL37, histone H3 and H4 allowed poly(C) and poly(A:U) to induce costimulation of naive CD4$^+$ T cells (Fig. 3f). These data indicated that NAs from self or pathogens could induce T-cell costimulation by forming complexes with antimicrobial peptides such as LL37 or core histones.

NA-mediated costimulation is independent of known sensors. To determine the mechanism of NA recognition and activation in T cells, we analysed the possible involvement of cytosolic sensors of NAs in innate cells. DNA-dependent activator of IRFs (DAI; also known as ZBP1) was first reported to function as a cytoplasmic DNA receptor[21]. Absent in melanoma 2 (AIM2) was identified as a cytosolic DNA sensor that activates inflammasome[22]. Stimulator of IFN genes (STING) and TBK1 have been identified as essential molecules that mediate a wide range of cytosolic DNA-induced type I IFN responses[23–25]. To examine the possible involvement of these sensors for T-cell costimulation, we tested naive CD4$^+$ T cells derived from *Zbp1*$^{-/-}$, *Asc*$^{-/-}$ (which links AIM2 to caspase-1), *Sting*$^{-/-}$ and *Tnf*$^{-/-}$ *Tbk1*$^{-/-}$ mice. However, surprisingly, DNA-mediated costimulation was induced normally in these T cells (Fig. 4a–c, Supplementary Fig. 3a), strongly suggesting that T cells utilize a DNA-sensing system different from innate immune cells.

TLR3 recognizes poly(I:C) in the endosome and initiates signalling through the adaptor, TRIF[1]. On the other hand, retinoic acid-inducible gene I (RIG-I) and melanoma differentiation-associated gene 5 (MDA5) sense poly(I:C) and viral RNA in the cytoplasm, which activates an adaptor, IFN-β promoter stimulator 1 (IPS-1; also known as MAVS)[26,27]. To examine the possibility that RIG-I/MDA5 and TLR3 may recognize RNA cooperatively or separately in T cells, we examined RNA-mediated T cell costimulation in IPS-1/TRIF-doubly deficient mice. Normal costimulation by poly(I:C) and poly(I) was observed in *Ips-1*$^{-/-}$ *Trif*$^{-/-}$ T cells (Fig. 4d). In addition, to determine the functional redundancy between TLRs and inflammasomes or RIG-I-like receptors (RLRs), we generated MyD88/ASC-and MyD88/IPS-1 doubly-deficient mice. NA-mediated costimulation was normally induced in naive CD4$^+$ T cells from both mutant mice (Supplementary Fig. 3b,c). It has been demonstrated that NAs are promiscuously sensed by HMGB proteins to induce type I IFN and pro-inflammatory cytokines[28]. However, downmodulation of all three HMGB proteins in CD4$^+$ T cells using small interfering RNA did not alter IL-2 production in response to NAs (Supplementary Fig. 3d).

To identify the mechanism underlying the NA-mediated costimulatory signal to induce IL-2 production in T cells, we

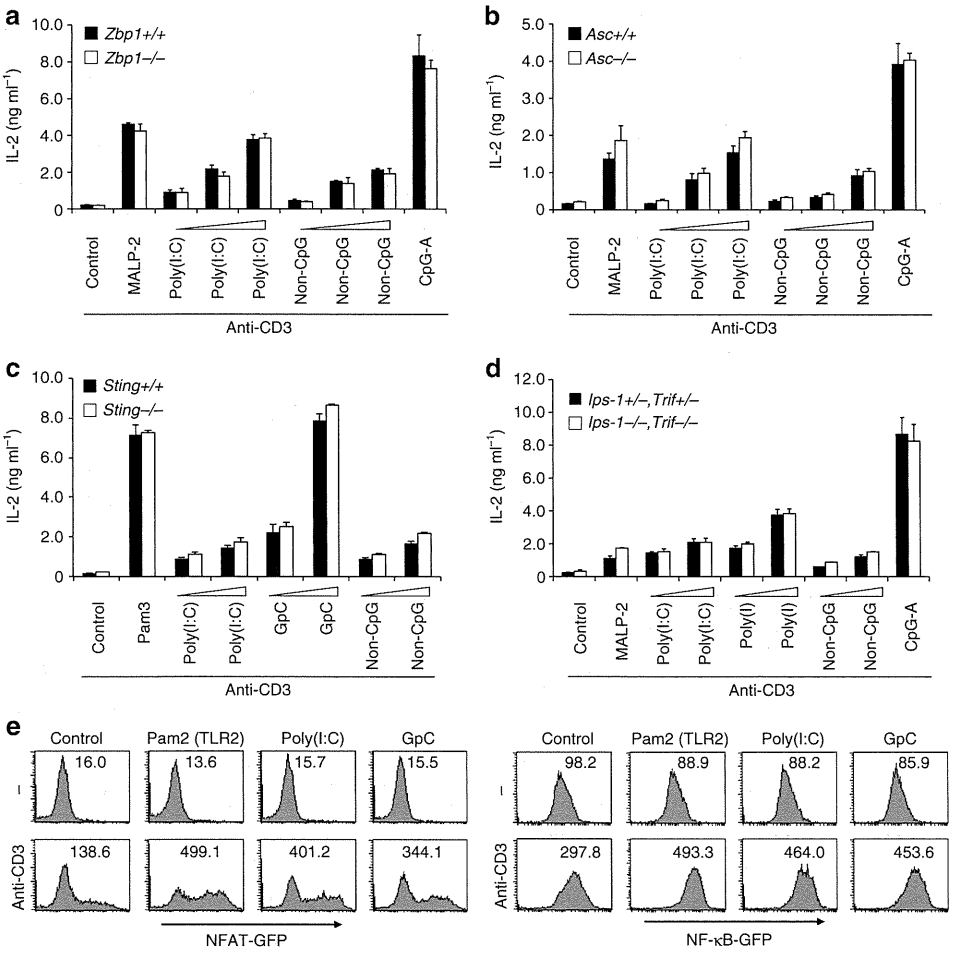

Figure 4 | NA-mediated T cell costimulation is independent of known innate sensors. (**a**–**d**) Naive CD4$^+$ T cells derived from WT or *Zbp1*$^{-/-}$ (**a**), *Asc*$^{-/-}$ (**b**), *Sting*$^{-/-}$ (**c**) or *Ips-1*$^{-/-}$ *Trif*$^{-/-}$ (**d**) mice were stimulated with plate-bound anti-CD3ε and the indicated ligands. After 48 h, IL-2 production was measured by ELISA. (**e**) T-cell hybridoma reporter cells expressing NFAT-GFP (left) or NF-κB-GFP (right) were stimulated with the indicated ligands with or without immobilized anti-CD3ε for 24 h and analysed by flow cytometry. Error bars indicate s.d. Data are representative of at least two independent experiments.

© 2014 Macmillan Publishers Limited. All rights reserved.

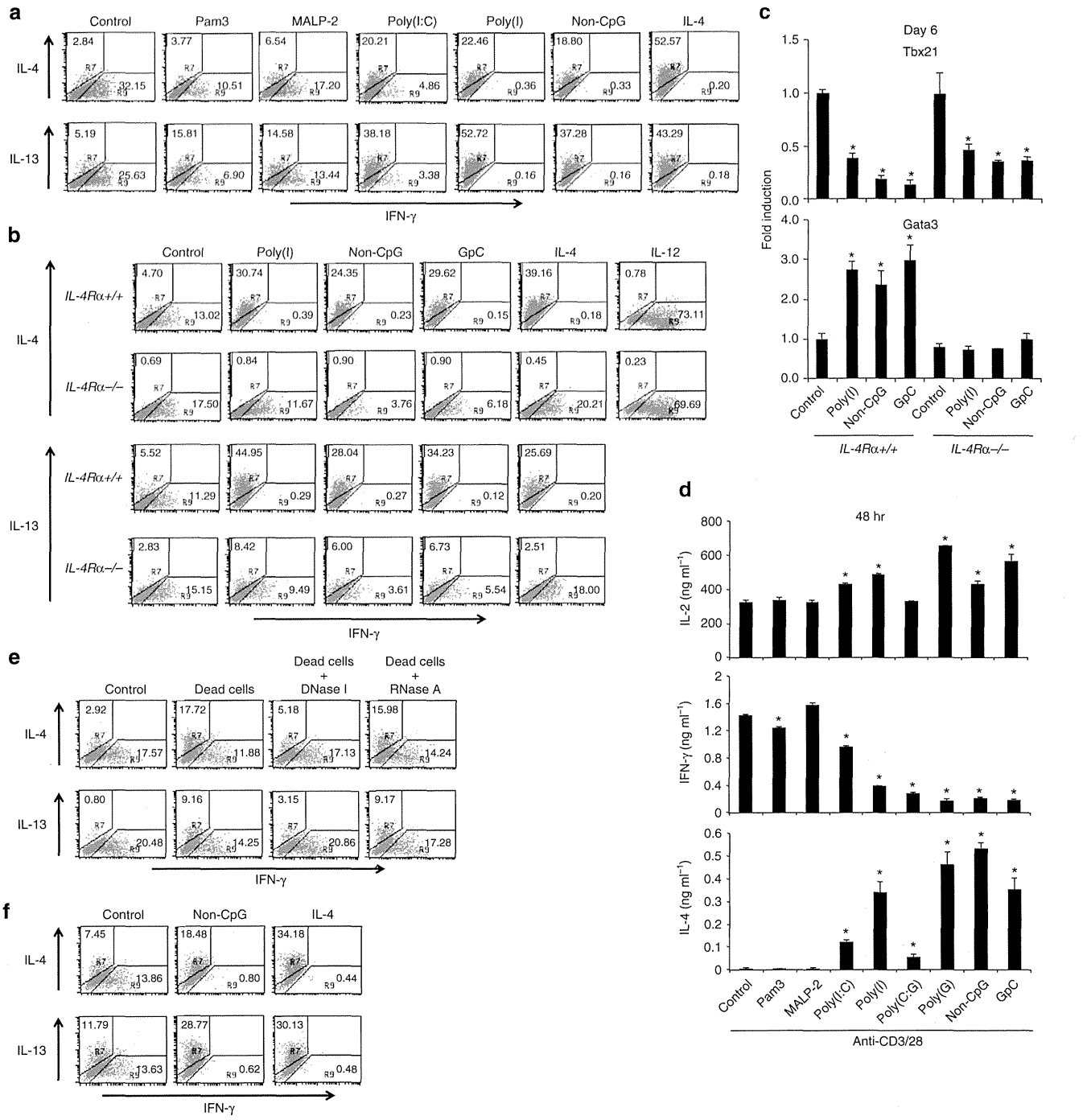

Figure 5 | NA-mediated costimulation induces Th2 differentiation. (**a**) Naive CD4$^+$ T cells were stimulated with immobilized anti-CD3ε (10 μg ml^{-1}) plus anti-CD28 (10 μg ml^{-1}) and the indicated ligands for 3 days, followed by culture with IL-2 (10 ng ml^{-1}) for an additional 3 days. Cells were subjected to real-time PCR analysis (**b**), or restimulated with immobilized anti-CD3ε plus anti-CD28 for 6 h for staining of intracellular cytokines IL-4 and IL-13. (**b**,**c**) Naive CD4$^+$ T cells from WT and IL-4Rα$^{-/-}$ mice were activated similarly as in (**a**) and cells were subjected to real-time PCR analysis (**c**) or restimulated with immobilized anti-CD3ε plus anti-CD28 for 6 h for staining of intracellular cytokines IL-4 and IL-13. *$P<0.05$, Student's *t*-test (compared with anti-CD3/CD28 plus non-CpG in WT cells). (**d**) Naive CD4$^+$ T cells were stimulated for 48 h with anti-CD3ε plus anti-CD28 and the indicated ligands and cytokine production was analysed by ELISA. *$P<0.05$, Student's *t*-test (compared with anti-CD3/CD28 alone). (**e**) Naive CD4$^+$ T cells with or without γ-irradiated naive CD4$^+$ T cells (Dead cells) at a 1:1 ratio were stimulated with anti-CD3ε plus anti-CD28 in the presence or absence of DNase I or RNase A, and analysed similarly as in (**a**). (**f**) Naive CD4$^+$ T cells from OT-II Tg mice were co-cultured with irradiated T cell-depleted splenocytes from C57BL/6 mice as APCs, together with OVA peptide (10 μM) in the presence or absence of non-CpG for 6 days. CD4$^+$ T cells were restimulated with immobilized anti-CD3ε plus anti-CD28 for 6 h for staining of intracellular cytokines. Error bars indicate s.d. Data are representative of at least three independent experiments.

analysed the activation of NF-κB and NFAT, both of which are essential for T-cell activation[29]. T-cell hybridoma (2B4) expressing the NF-κB-GFP or NFAT-GFP was stimulated by NAs plus anti-CD3. We observed that poly(I:C) and GpC markedly increased activation of NF-κB and NFAT, compared with anti-CD3 alone (Fig. 4e). These data suggest that enhanced

© 2014 Macmillan Publishers Limited. All rights reserved.

activation of NF-κB and NFAT is involved in the induction of NA-mediated T-cell costimulation. It is also worth noting that NA-induced costimulation of a T-cell hybridoma, which is definitely free of any innate cells, confirms that NA directly stimulates T cells.

NA-mediated costimulation induces Th2 cell differentiation. A recent study demonstrated that DNA released from dying host cells stimulates Th2 responses *in vivo*[30]. It is also reported that stimulation of RLRs by specific ligands biases the immune system toward a Th2 response, whereas the TLR signalling strongly induces Th1 and Th17 responses[31]. Accordingly, it seemed possible that NA-induced stimulation of T cells would induce Th2 cell differentiation. To test this hypothesis, naive $CD4^+$ T cells were stimulated *in vitro* with anti-CD3 plus anti-CD28 together with various NAs without blocking Abs against IFN-γ or IL-4. NAs such as poly(I:C), poly(I) and non-CpG strongly induced the differentiation of IL-4-producing T cells without the addition of exogenous IL-4 (Fig. 5a). By contrast, NAs strongly inhibited the differentiation of IFN-γ-producing T cells (Fig. 5a), and also increased the frequency of Th2 cells producing IL-5, IL-9, IL-13 and IL-10 (Fig. 5a, Supplementary Fig. 4a). Consistently, the expression of the Th2-master regulator GATA-3 was enhanced, whereas the expression of T-bet, the Th1-master regulator was strongly inhibited in the T cells cultured with NAs (Supplementary Fig. 4b), suggesting that NAs directly induce the differentiation of Th2 cells. Notably, unlike NAs, TLR2 ligands had a minimal effect on Th1 and Th2 differentiation (Fig. 5a), and NA-mediated costimulation did not affect the development of IL-17-producing T cells (Supplementary Fig. 4c). Since NAs induced Th2 differentiation of MyD88/TRIF-double deficient T cells similarly to control T cells (Supplementary Fig. 4d), this processes does not require TLR signalling.

The generation of Th2 cells is dependent on IL-4–STAT6 signalling, which leads to the upregulation of GATA-3 (ref. 32). We assessed whether Th2 differentiation induced by NA-mediated costimulation was also IL-4–STAT6-dependent. IL-4 receptor (R) α-deficient T cells after activation by NAs for 6 days failed to produce any Th2 cytokines including IL-4 and IL-13 (Fig. 5b). In addition, the induction of GATA-3 expression was severely diminished in IL-4Rα-deficient T cells (Fig. 5c). Similar results were obtained using *Stat6*$^{-/-}$ $CD4^+$ T cells (Supplementary Fig. 4e), indicating that NA-mediated Th2 differentiation requires IL-4–STAT6 signalling. However, NA-mediated inhibition of IFN-γ production and T-bet expression was still observed in IL-4Rα-deficient T cells (Fig. 5b,c), suggesting that NA-mediated inhibition of Th1 differentiation is independent of IL-4 signalling. Therefore, it is likely that NA-mediated costimulation may enhance IL-4 production at an early time point (within 48 h), which then induces Th2 differentiation. Indeed, IL-4 production was induced at 48 h by NAs but not TLR2 ligands, whereas IFN-γ production was reduced (Fig. 5d). NA-induced enhancement of IL-2 production was not strong upon stimulation with anti-CD3 plus CD28 as compared with anti-CD3 alone. Strong costimulation with anti-CD28 resulted in reduced enhancement, though significantly enhanced (Fig. 5d).

Collectively, these data demonstrate that NAs induce Th2 differentiation in an IL-4 signal-dependent manner similarly to the canonical Th2 differentiation pathway induced by exogenous IL-4, whereas suppression of Th1 differentiation by NAs is independent of IL-4 signalling.

We next determined whether self-DNA from dead cells induce Th2 differentiation. We found that the addition of dead cells (irradiated naive $CD4^+$ T cells or irradiated HEK 293 cells) to the T-cell culture enhanced the differentiation of IL-4-producing cells, which was cancelled by the addition of DNase I into the medium (Fig. 5e, Supplementary Fig. 5f). Addition of RNase A resulted in minimal effect. These data suggest that self-DNA is a critical factor for Th2 differentiation induced by dead cells. To examine whether NA-mediated Th2 differentiation is induced upon antigen stimulation, OVA-specific naive CD4+ T cells from OT-II Tg mice were stimulated with OVA peptide-pulsed irradiated splenocytes plus non-CpG. Non-CpG promoted Th2 differentiation under the condition, strongly suggesting that NAs induces T-cell costimulation even when T cells are activated by antigen-pulsed APCs (Fig. 5f).

Mechanisms underlying NA-induced Th2 differentiation. To determine the mechanism by which NAs induces Th2 differentiation, we compared the gene expression profiles in $CD4^+$ T cells activated under neutral conditions in the presence or absence of non-CpG. Surprisingly, before the upregulation of GATA-3, the expression of T-bet was strongly inhibited by non-CpG-mediated costimulation (Fig. 6a). Following the suppression of T-bet expression, the expression of Th2-associated genes was upregulated and IFN-γ was downregulated at 48 h after stimulation (Fig. 6a). We further confirmed that various NAs other than non-CpG also induced the suppression of T-bet and the upregulation of GATA-3 and IL-4 expression (Supplementary Fig. 5a). We then compared the kinetics of the expression of Th1/Th2-associated genes upon stimulation with IL-4 or non-CpG. GATA-3 was quickly induced in $CD4^+$ T cells by exogenous IL-4 (at 24 h), followed by the induction of Th2 cytokines and the inhibition of T-bet and IFN-γ expression. By contrast, in $CD4^+$ T cells stimulated with non-CpG, GATA-3 expression was induced after inhibition of T-bet expression, suggesting that Th2-associated genes are indirectly induced by non-CpG-mediated costimulation. In addition to these kinetic differences, inhibition of T-bet expression by non-CpG was more rapid and robust than by exogenous IL-4 (Fig. 6b). T-bet inhibits Th2 differentiation by directly inhibiting the expression of Th2 cytokines and sequestering GATA-3 from the promoters of Th2 cytokines[33]. Using ChIP analysis, we showed that the binding of GATA-3 to the IL-4 and IL-13 promoters was enhanced in $CD4^+$ T cells by stimulation with non-CpG (Fig. 6c). Therefore, it is likely that NA-mediated costimulation induces Th2 differentiation primarily by inhibiting T-bet expression.

To test this hypothesis further, we compared Th2 differentiation by the blockade of IFN-γ signalling and non-CpG stimulation, because the expression of T-bet is controlled by IFN-γ signalling[34]. We found that the T-bet expression in $CD4^+$ T cells cultured in the presence of anti-IFN-γ was much lower than those stimulated with non-CpG at early time point (48 h) after TCR stimulation (Fig. 6d). However, the expression of GATA-3 and Th2 cytokines in T cells cultured with anti-IFN-γ was much lower than those stimulated with non-CpG (Fig. 6d), suggesting that inhibition of T-bet expression by non-CpG is not sufficient, though partially contributes, for the upregulation of Th2-associated gene expression. Additional signal(s) are required for the induction of Th2-associated genes by non-CpG-mediated costimulation. Consistently, the Th2 polarization by the presence of anti-IFN-γ was weaker than by non-CpG later (day 6) after TCR priming (Fig. 6e). Thus, non-CpG-mediated costimulation simultaneously inhibits T-bet expression and enhances the expression of Th2-associated genes.

As T-bet controls Th1 development by directly activating IFN-γ (ref. 34), it is likely that NA-mediated costimulation would inhibit Th1 development under Th1-polarizing conditions. As expected, non-CpG inhibits Th1 development and

© 2014 Macmillan Publishers Limited. All rights reserved.

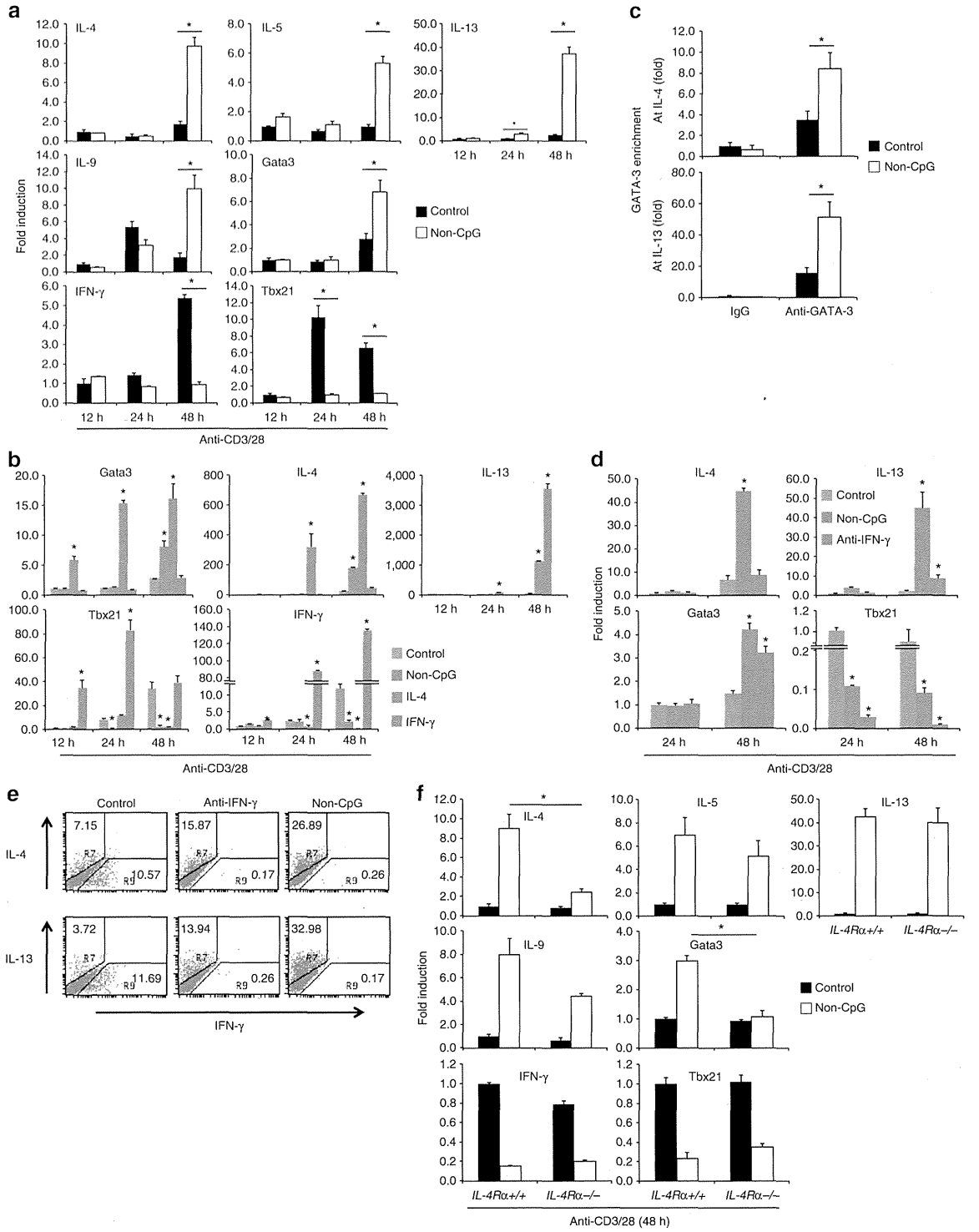

Figure 6 | Molecular mechanism of NA-mediated Th2 differentiation. (**a**) Naive CD4$^+$ T cells were stimulated with anti-CD3ε plus anti-CD28 with or without non-CpG for the indicated periods and mRNA expression was analysed by real-time PCR. *$P<0.01$, Student's *t*-test (compared with anti-CD3/CD28 alone). (**b**) Naive CD4$^+$ T cells were stimulated by NAs or IL-4 and analysed similarly in (**a**). *$P<0.01$, Student's *t*-test (compared with anti-CD3/CD28 alone). (**c**) Naive CD4$^+$ T cells were stimulated with anti-CD3ε plus anti-CD28 together with non-CpG for 48 h, and ChIP analyses were performed by immunoprecipitation with control Ab (IgG) or anti-GATA-3. Quantitative PCR analysis of the GATA3 binding at the IL-4 and IL-13 gene promoters. The results were normalized to those of a standardized aliquot of input chromatin. *$P<0.05$, Student's *t*-test (compared with anti-CD3/CD28 alone). (**d**,**e**) Naive CD4$^+$ T cells were stimulated in the presence of non-CpG or anti-IFN-γ Ab and mRNA expression (**d**) and intracellular cytokine expression (day 6) (**e**) were analysed. *$P<0.01$, Student's *t*-test (compared with anti-CD3/CD28 alone). (**f**) Naive CD4$^+$ T cells from WT and IL-4Rα$^{-/-}$ mice were stimulated and analysed similarly in (**a**). *$P<0.01$, Student's *t*-test (compared with anti-CD3/CD28 plus non-CpG in WT cells). Error bars indicate s.d. Data are representative of at least two independent experiments.

© 2014 Macmillan Publishers Limited. All rights reserved.

IFN-γ production even under Th1 differentiation condition (Supplementary Fig. 5b).

We then analysed whether IL-4 signalling is required for the early expression of Th2-associated genes after NA-mediated costimulation. Interestingly, the augmentation of the expression of IL-4 and GATA-3 by non-CpG was severely impaired in IL-4Rα-deficient CD4$^+$ T cells, whereas the upregulation of IL-5, IL-9 and IL-13 expression and downregulation of IFN-γ and T-bet expression was largely unaffected (Fig. 6f). Similar results were obtained in the *Stat6*$^{-/-}$ CD4$^+$ T cells (Supplementary Fig. 5c). These data suggest that non-CpG-mediated T-cell costimulation directly induced the expression of IL-5, IL-9 and IL-13, partly through the inhibition of T-bet expression, whereas IL-4 and GATA-3 expression was induced by IL-4–STAT6 signalling. Naive CD4$^+$ T cells are capable of producing IL-4 upon primary TCR stimulation in the absence of exogenous IL-4, and the early IL-4 is rapidly consumed by the CD4$^+$ T cells themselves[35]. Therefore, NA-mediated IL-4 production may require early IL-4 autocrine signalling to induce the autoactivation of GATA-3 expression. Notably, however, expression of all Th2-associated genes in IL-4Rα-deficient CD4$^+$ T cells disappeared by day 6 after priming with NAs. Although non-CpG stimulation induces the enrichment of GATA-3 on the IL-13 promoter (Fig. 6c), it seems that early induction of IL-13 expression by non-CpG (at 48 h) is independent of GATA-3 because IL-13 expression was enhanced by non-CpG in IL-4Rα-deficient CD4$^+$ T cells despite the lack of GATA-3 upregulation by non-CpG (Fig. 6f). However, it seems that the enrichment of GATA-3 on the IL-13 promoter is critical for IL-13 expression later (in day 6) after TCR priming for its maintenance because the induction of IL-13 and GATA-3 expression by non-CpG was diminished later after TCR priming (in day 6) in IL-4Rα-deficient CD4$^+$ T cells (Fig. 5b,c). These data indicate that autocrine IL-4 is required for the induction of IL-4 and GATA-3 upon non-CpG stimulation, which then acts to amplify and stabilize the expression of Th2-associated genes.

Discussion

The present study shows that NAs directly stimulate CD4$^+$ T cells through a NA sensor different from those of the innate system, subsequently leading to Th2 cell differentiation. In addition to TLRs, a growing number of NA sensors have been identified in the innate immune system, including RLRs, IPS-1-dependent sensors, MyD88/TRIF-dependent sensors, ASC-dependent inflammasomes and STING-dependent sensors[36]. However, we found that recognition of NAs by T cells is independent of all of these known sensors including HMGBs, although we cannot conclusively exclude the possibility that some known NA sensors work redundantly.

We found that a higher-order structure of the NAs is required for their incorporation by T cells. Since T cells can incorporate genomic self-DNA only when it is complexed with antimicrobial peptides or core histones, T cells may respond to NAs from dying cells at the site of inflammation and infection, where antimicrobial peptides and/or histones are released. We also demonstrated that specific recognition and uptake of RNA induces costimulatory responses. A recent study demonstrated that cells infected with several viruses including vaccinia virus contained higher-order structured RNA that stimulated MDA5 (ref. 37), indicating the possibility that T cells may recognize such viral RNA and are activated. Recent studies demonstrated that, upon infection with nonpermissive HIV, cytoplasmic DNA derived from incomplete reverse transcripts caused CD4$^+$ T cell death through recognition of the cytosolic DNA by a sensor IFI16 followed by activation of the ASC-caspase-1 pathway[38,39]. It was also reported that transfected DNA was colocalized with IFI16 in activated T cells[40]. However, our result that DNA-mediated costimulation was normally induced in ASC-deficient CD4$^+$ T cells suggests that IFI16 is not involved in the DNA-mediated costimulation in T cells. While cytosolic DNA stimulates IFI16 upon HIV infection or DNA transfection, incorporated DNAs are accumulated in endosome/lysosome and induce T-cell costimulation in our experiments without activation of IFI16 probably due to the failure to deliver DNA to the cytosol.

Furthermore, a recent study showed that immunization with RLR ligands or infection with viruses, which mainly activate RLRs, results in enhanced Th2 responses and much weaker Th1 responses[31], supporting our observation that NAs directly stimulate the induction of Th2 responses. It is known that TLR stimulation of innate immune cells promotes Th1 and Th17 responses by inducing the Th1-polarizing cytokine IL-12 and the Th17-polarizing cytokines IL-6/IL-23/IL-1 (refs 1,41). Recent studies, including ours, show that TLR2 ligands directly activate Th1 but not Th2 cells[7] and promote Th17 differentiation[8]. In contrast to TLR, the activation of RLRs suppresses Th1 and Th17 differentiation through the inhibition of IL-12 and IL-23 production, resulting in the enhanced differentiation of Th2 cells[31]. Our results demonstrate that direct stimulation of T cells by NAs strongly inhibit the initial expression of T-bet, which allows the initial production of IL-4 and Th2 cytokines to induce Th2 differentiation. Thus, similar to Th1 and Th17 responses induced by TLRs in innate cells and T cells, it is likely that activation of RLRs in innate cells and the NA sensor in T cells by NAs cooperatively induces Th2 differentiation.

The initial origin of IL-4 to trigger Th2 differentiation has been extensively analysed but remains unclear. It has been reported that basophils serve as Th2 cell-promoting APCs by producing IL-4 and/or thymic stromal lymphopoietin[14]. However, their role as APCs remains controversial[42]. It has been suggested that naive T cells are a possible source of IL-4 (refs 43,44), which modestly induces Th2 differentiation when IFN-γ and IL-12 are neutralized[35]. Although it has been proposed that Th2 differentiation may occur as a default pathway, CD4$^+$ T cells in IL-12 p40-deficient mice fail to differentiate into Th2 cells in response to intracellular pathogens[45]. Thus, the simple blocking of Th1-inducing stimuli such as IL-12 or IFN-γ is not sufficient to induce Th2 differentiation, suggesting the existence of additional Th2-inducing factors. However, such factors for the initial triggering of IL-4 production from naive CD4$^+$ T cells under physiological conditions have not been identified. We here provide strong evidence that the initial IL-4 production derived from naive CD4$^+$ T cells upon recognition of NAs in the absence of any exogenous cytokines or neutralizing antibodies instructs naive CD4$^+$ T cells to differentiate into Th2 cells.

A recent report demonstrated that aluminium hydroxide adjuvant (alum) causes cell death and release of host DNA at sites of immunization, which mediates the adjuvant effect for Th2-biased adaptive responses[30]. As the mechanism to induce Th2 responses, it has been reported that uric acid released in the peritoneal cavity after injection of alum may have a role in promoting Th2 cell responses independently of the ASC inflammasome or TLR signalling[46]. As uric acid crystals released at the sites of immunization/inflammation induce extracellular DNA traps formation by neutrophil, eosinophil and basophil[47], uric acid-induced extracellular DNA traps may directly stimulate T cells to induce Th2 response. A recent study reported that defects in clearance of apoptotic airway epithelial cells upon environmental allergen encounter lead to augmented Th2 cytokine production and airway hyper-responsiveness[48], indicating that *in vivo* Th2 responses are closely related to host

© 2014 Macmillan Publishers Limited. All rights reserved.

cell death accompanied by host DNA release. In line with the hypothesis, we found that self-DNA from dead cells induces Th2 differentiation.

Collectively, we have identified NAs as a direct Th2-inducing factor, which induces initial production of IL-4 by naive $CD4^+$ T cells, which in turn induces Th2 differentiation. Although we have not identified the NAs sensor in T cells yet, our results provide the possibility that NAs may be critical targets for the development of improved vaccine adjuvants and the overall design of therapeutics to control allergic diseases.

Methods

Mice. C57BL/6 mice were purchased from Clea Japan, Inc. The mice deficient in MyD88, TRIF-deficient, IPS-1 ZBP1 and STAT6 were provided by Dr Akira S. *Asc*$^{-/-}$ mice were provided by Dr Taniguchi S and Dr Noda T. *Sting*$^{-/-}$ and *Il4ra*$^{-/-}$ mice were provided by Dr Barber GN and Dr Brombacher F, respectively. Mice aged 8–16 weeks were used. All mice were maintained under specific pathogen-free conditions and all experiments were conducted under protocols approved by RIKEN Yokohama Institute.

ELISA and cell growth analysis. Cell culture supernatants were analysed by ELISA for the production of IL-2 (BD biosciences), IL-4 (BD biosciences) and IFN-γ (BD biosciences). Cell growth was assessed by the MTS assay-based Cell Counting Kit-8 (DOJINDO).

Helper T-cell differentiation. $CD4^+/CD25^-/CD62L^+/NK1.1^-$ (naive) T cells were isolated from spleens using a FACS-Aria cell sorter. For Th0 cells, cells were stimulated with plate-bound anti-CD3 (2C11, 10 μg ml^{-1}) and anti-CD28 (PV-1, 10 μg ml^{-1}) Abs in the presence of the indicated ligands. For Th1 cells, cells were cultured in the presence of IL-12 (10 ng ml^{-1}) and anti-IL-4 Abs (10 μg ml^{-1}). For Th2 cells, cells were similarly cultured in the presence of IL-4 (10 ng ml^{-1}).

Real-time quantitative PCR. After removal of genomic DNA by treatment with DNase (Wako Nippon Gene), randomly primed cDNA strands were generated with reverse transcriptase II (Invitrogen). RNA expression was quantified by real-time PCR with the following gene-specific primers and values were normalized to the expression of *Rps18* mRNA (Supplementary Table 2).

Reagents and Abs. The TLR2 ligands *N*-palmitoyl-*S*-(2,3-bis(palmitoyloxy)-(2*RS*)-propyl)-Cys-Ser-Lys_4 (Pam3) and macrophage-activating lipopeptide 2 (MALP-2) were purchased from EMC Microcollections. Poly(I:C), a TLR3 ligand, and LPS (*Escherichia. coli* O111:B4), a TLR4 ligand, were obtained from GE Healthcare Biosciences and Sigma, respectively. Flagellin, a TLR5 ligand, and loxoribine, a TLR7 ligand, were obtained from InvivoGen. Oligo DNAs including TLR9 ligands were purchased from Hokkaido System Science. Poly(A), poly(U), poly(C), poly(G), poly(I), poly(A:U) and poly(C:G) were purchased from Sigma. Calf thymus DNA and *E. coli* DNA was from Sigma and Invivogen, respectively. LL37 was from AnaSpec. Histone H1, H2A, H2B, H3 and H4 were from New England BioLabs. LL37 or histones were first premixed with genomic DNA (peptide:DNA mass ratio of 2:1). After 30-min incubation at room temperature, the mix was added to the T-cell cultures (final concentration was 10 μg ml^{-1} of DNA).

Abs specific for anti-IL-4 PE (11B11, 1:25 dilution) and anti-IFN-γ FITC (XMG1.2, 1:25 dilution) were obtained from BD Biosciences; anti-IL-5 PE (TRFK5, 1:25 dilution), anti-IL-10 PE (1:25 dilution) and anti-IL-13 PE (eBio13A, 1:25 dilution) from eBioscience; anti-IL-9 PE (RM9A4, 1:25 dilution) from BioLegend. ChIP analysis used mAb to GATA-3 (HG3-31AC; Santa Cruz, 1:125 dilution).

Intracellular cytokine staining analysis. $CD4^+$ T cells were restimulated with immobilized anti-CD3 and anti-CD28 for 6 h in the presence of 2 μM monensin (Sigma, St Louis, MO). Cells were fixed with 4% paraformaldehyde and permeabilized with 0.5% Triton X-100. After blocking with 3% BSA-PBS, cells were stained with antibodies to each cytokine. Flow cytometric analysis was performed on a FACSCalibur and data were analysed with BD CellQuest.

Cellular uptake of NA. To analyse the uptake of NA, 2×10^5 cells were pre-incubated at 37 °C for 10 min in medium. Cells were incubated with fluorescence-labelled NA at 37 °C for 90 min. Then cells were washed once in HANKS/0.1% BSA followed by an acidic wash with 100 mM acetic acid, 150 mM NaCl (pH2.7) for 1 min to remove unbound and cell surface-bound NA. Subsequently, cells were washed two times in HANKS/0.1% BSA, and were analysed by flow cytometry using the FACSCalibur.

Reporter cells. The 2B4-NFAT-GFP cells have been described[49] and the 2B4-NF-κB-GFP cells were established by transfection of NF-κB-GFP into 2B4 hybridoma cells. These cells were cultured in RPMI 1640 medium supplemented with 10% (vol/vol) FCS and β-mercaptoethanol.

Chromatin immunoprecipitation assay. Cells were fixed for 10 min at 4 °C with 10% formaldehyde. After incubation, glycine was added to a final concentration of 0.125 M to quench the formaldehyde. Cells were pelleted, washed three times with ice-cold PBS and then lysed. The lysates were sonicated to reduce DNA length to between 200 and 300 base pairs. The chromatin was pre-cleared with protein G agarose beads for 6 h and then incubated with 4 μg of anti-GATA-3 (HG3-31) agarose conjugate antibody (Santa Cruz, sc-268 AC) or control IgG overnight. The precipitates were washed and eluted in 120 μl of $NaHCO_3$ buffer with 1% SDS. The samples were treated with RNase and Proteinase K and then de-crosslinked at 65 °C overnight. Precipitated DNA was further purified with Qiaquick PCR purification kit (Qiagen) and was analysed by quantitative PCR (Supplementary Table 2)[50].

Confocal microscopic imaging. Cells were settled on glass-bottom, 35-mm tissue culture dishes (MATSUNAMI GLASS). Confocal microscopy analyses were performed with a Leica TCS SP5 confocal microscope with an oil immersion objective (HCX PL APO × 63/1.40–0.60 NA, Leica). Dual-color images were acquired using a sequential acquisition mode to avoid cross-excitation. To visualize the Histone–calf thymus DNA complex in $CD4^+$ T cells, calf thymus DNA (Sigma) was labelled with Cy5 using the Label IT Nucleic Acid Labelling Reagents (Mirus) and histone H3 was labelled with DyLight 488 using the antibody labelling kit (Pierce), according to the standard protocol provided by the respective manufacturers.

RNA interference. Double-stranded oligonucleotides corresponding to the target sequences were cloned into the pSuper.Retro RNAi plasmid (OligoengineInc.). The siRNA targeting sequences which function for commonly all three murine HMGB1/2/3 are 5′-GAGAAGTATGAGAAGGATATT-3′ and 5′-AAGTATGAGA AGGATATTGCT-3′.

Statistics. Statistical significance was determined by a two-tailed unpaired Student's *t*-test. $P<0.05$ was considered statistically significant.

References

1. Takeda, K., Kaisho, T. & Akira, S. Toll-like receptors. *Annu. Rev. Immunol.* **21,** 335–376 (2003).
2. Medzhitov, R. Toll-like receptors and innate immunity.. *Nat. Rev. Immunol.* **1,** 135–145 (2001).
3. Komai-Koma, M., Jones, L., Ogg, G. S., Xu, D. & Liew, F. Y. TLR2 is expressed on activated T cells as a costimulatory receptor. *Proc. Natl Acad. Sci. USA* **101,** 3029–3034 (2004).
4. Cottalorda, A. *et al.* TLR2 engagement on CD8 T cells lowers the threshold for optimal antigen-induced T cell activation. *Eur. J. Immunol.* **36,** 1684–1693 (2006).
5. Sutmuller, R. P. *et al.* Toll-like receptor 2 controls expansion and function of regulatory T cells. *J. Clin. Invest.* **116,** 485–494 (2006).
6. Liu, H., Komai-Koma, M., Xu, D. & Liew, F. Y. Toll-like receptor 2 signaling modulates the functions of CD4+ CD25+ regulatory T cells. *Proc. Natl Acad. Sci. U. S. A.* **103,** 7048–7053 (2006).
7. Imanishi, T. *et al.* Cutting edge: TLR2 directly triggers Th1 effector functions. *J. Immunol.* **178,** 6715–6719 (2007).
8. Reynolds, J. M. *et al.* Toll-like receptor 2 signaling in CD4(+) T lymphocytes promotes T helper 17 responses and regulates the pathogenesis of autoimmune disease. *Immunity* **32,** 692–702 (2010).
9. Caron, G. *et al.* Direct stimulation of human T cells via TLR5 and TLR7/8: flagellin and R-848 up-regulate proliferation and IFN-gamma production by memory CD4+ T cells. *J. Immunol.* **175,** 1551–1557 (2005).
10. Gelman, A. E. *et al.* The adaptor molecule MyD88 activates PI-3 kinase signaling in CD4+ T cells and enables CpG oligodeoxynucleotide-mediated costimulation. *Immunity* **25,** 783–793 (2006).
11. Gelman, A. E., Zhang, J., Choi, Y. & Turka, L. A. Toll-like receptor ligands directly promote activated CD4+ T cell survival. *J. Immunol.* **172,** 6065–6073 (2004).
12. Peng, G. *et al.* Toll-like receptor 8-mediated reversal of CD4+ regulatory T cell function. *Science* **309,** 1380–1384 (2005).
13. Zhu, J., Yamane, H. & Paul, W. E. Differentiation of effector CD4 T cell populations (*). *Annu. Rev. Immunol.* **28,** 445–489 (2010).
14. Paul, W. E. & Zhu, J. How are T(H)2-type immune responses initiated and amplified? *Nat. Rev. Immunol.* **10,** 225–235 (2010).
15. Kerkmann, M. *et al.* Spontaneous formation of nucleic acid-based nanoparticles is responsible for high interferon-alpha induction by CpG-A in plasmacytoid dendritic cells. *J. Biol. Chem.* **280,** 8086–8093 (2005).
16. Bishop, J. S. *et al.* Intramolecular G-quartet motifs confer nuclease resistance to a potent anti-HIV oligonucleotide. *J. Biol. Chem.* **271,** 5698–5703 (1996).

© 2014 Macmillan Publishers Limited. All rights reserved.

17. Dalpke, A. H., Zimmermann, S., Albrecht, I. & Heeg, K. Phosphodiester CpG oligonucleotides as adjuvants: polyguanosine runs enhance cellular uptake and improve immunostimulative activity of phosphodiester CpG oligonucleotides *in vitro* and *in vivo*. *Immunology* **106,** 102–112 (2002).
18. Arnott, S., Chandrasekaran, R. & Marttila, C. M. Structures for polyinosinic acid and polyguanylic acid. *Biochem. J.* **141,** 537–543 (1974).
19. Lande, R. *et al.* Plasmacytoid dendritic cells sense self-DNA coupled with antimicrobial peptide. *Nature* **449,** 564–569 (2007).
20. Mantovani, A., Cassatella, M. A., Costantini, C. & Jaillon, S. Neutrophils in the activation and regulation of innate and adaptive immunity. *Nat. Rev. Immunol.* **11,** 519–531 (2011).
21. Takaoka, A. *et al.* DAI (DLM-1/ZBP1) is a cytosolic DNA sensor and an activator of innate immune response. *Nature* **448,** 501–505 (2007).
22. Hornung, V. *et al.* AIM2 recognizes cytosolic dsDNA and forms a caspase-1-activating inflammasome with ASC. *Nature* **458,** 514–518 (2009).
23. Ishikawa, H. & Barber, G. N. STING is an endoplasmic reticulum adaptor that facilitates innate immune signalling. *Nature* **455,** 674–678 (2008).
24. Ishikawa, H., Ma, Z. & Barber, G. N. STING regulates intracellular DNA-mediated, type I interferon-dependent innate immunity. *Nature* **461,** 788–792 (2009).
25. Ishii, K. J. *et al.* A Toll-like receptor-independent antiviral response induced by double-stranded B-form DNA. *Nat. Immunol.* **7,** 40–48 (2006).
26. Kato, H. *et al.* Length-dependent recognition of double-stranded ribonucleic acids by retinoic acid-inducible gene-I and melanoma differentiation-associated gene 5. *J. Exp. Med.* **205,** 1601–1610 (2008).
27. Kawai, T. *et al.* IPS-1, an adaptor triggering RIG-I- and Mda5-mediated type I interferon induction. *Nat. Immunol.* **6,** 981–988 (2005).
28. Yanai, H. *et al.* HMGB proteins function as universal sentinels for nucleic-acid-mediated innate immune responses. *Nature* **462,** 99–103 (2009).
29. Smith-Garvin, J. E., Koretzky, G. A. & Jordan, M. S. T cell activation. *Annu. Rev. Immunol.* **27,** 591–619 (2009).
30. Marichal, T. *et al.* DNA released from dying host cells mediates aluminum adjuvant activity. *Nat. Med.* **17,** 996–1002 (2011).
31. Negishi, H. *et al.* Cross-interference of RLR and TLR signaling pathways modulates antibacterial T cell responses. *Nat. Immunol.* **13,** 659–666 (2012).
32. Zheng, W. & Flavell, R. A. The transcription factor GATA-3 is necessary and sufficient for Th2 cytokine gene expression in CD4 T cells. *Cell* **89,** 587–596 (1997).
33. Hwang, E. S., Szabo, S. J., Schwartzberg, P. L. & Glimcher, L. H. T helper cell fate specified by kinase-mediated interaction of T-bet with GATA-3. *Science* **307,** 430–433 (2005).
34. Afkarian, M. *et al.* T-bet is a STAT1-induced regulator of IL-12R expression in naive CD4+ T cells. *Nat. Immunol.* **3,** 549–557 (2002).
35. Noben-Trauth, N., Hu-Li, J. & Paul, W. E. Conventional, naive CD4+ T cells provide an initial source of IL-4 during Th2 differentiation. *J. Immunol.* **165,** 3620–3625 (2000).
36. Desmet, C. J. & Ishii, K. J. Nucleic acid sensing at the interface between innate and adaptive immunity in vaccination. *Nat. Rev. Immunol.* **12,** 479–491 (2012).
37. Pichlmair, A. *et al.* Activation of MDA5 requires higher-order RNA structures generated during virus infection. *J. Virol.* **83,** 10761–10769 (2009).
38. Monroe, K. M. *et al.* IFI16 DNA sensor is required for death of lymphoid CD4 T cells abortively infected with HIV. *Science* **343,** 428–432 (2014).
39. Doitsh, G. *et al.* Cell death by pyroptosis drives CD4 T-cell depletion in HIV-1 infection. *Nature* **505,** 509–514 (2014).
40. Berg, R. K. *et al.* T cells detect intracellular DNA but fail to induce Type I IFN responses: implications for restriction of HIV replication. *PloS One* **9,** e84513 (2014).
41. Goriely, S., Neurath, M. F. & Goldman, M. How microorganisms tip the balance between interleukin-12 family members. *Nat. Rev. Immunol.* **8,** 81–86 (2008).
42. Kim, S. *et al.* Cutting edge: basophils are transiently recruited into the draining lymph nodes during helminth infection via IL-3, but infection-induced Th2 immunity can develop without basophil lymph node recruitment or IL-3. *J. Immunol.* **184,** 1143–1147 (2010).
43. Yagi, R. *et al.* The IL-4 production capability of different strains of naive CD4(+) T cells controls the direction of the T(h) cell response. *Int. Immunol.* **14,** 1–11 (2002).
44. Liu, Z. *et al.* IL-2 and autocrine IL-4 drive the *in vivo* development of antigen-specific Th2 T cells elicited by nematode parasites. *J. Immunol.* **174,** 2242–2249 (2005).
45. Jankovic, D. *et al.* In the absence of IL-12, CD4(+) T cell responses to intracellular pathogens fail to default to a Th2 pattern and are host protective in an IL-10(-/-) setting. *Immunity* **16,** 429–439 (2002).
46. Kool, M. *et al.* An unexpected role for uric acid as an inducer of T helper 2 cell immunity to inhaled antigens and inflammatory mediator of allergic asthma. *Immunity* **34,** 527–540 (2011).
47. Schorn, C. *et al.* Monosodium urate crystals induce extracellular DNA traps in neutrophils, eosinophils, and basophils but not in mononuclear cells. *Front. Immunol.* **3,** 277 (2012).
48. Juncadella, I. J. *et al.* Apoptotic cell clearance by bronchial epithelial cells critically influences airway inflammation. *Nature* **493,** 547–551 (2013).
49. Ohtsuka, M. *et al.* NFAM1, an immunoreceptor tyrosine-based activation motif-bearing molecule that regulates B cell development and signaling. *Proc. Natl Acad. Sci. USA* **101,** 8126–8131 (2004).
50. Tanaka, S. *et al.* The enhancer HS2 critically regulates GATA-3-mediated Il4 transcription in T(H)2 cells. *Nat. Immunol.* **12,** 77–85 (2011).

Acknowledgements

We thank S. Yamasaki, T. Yokosuka, S. Tsukumo, A. Takeuchi, R. Onishi, H. Ike, Y. Motomura and M. Kubo for discussions and experimental help, M. Sakuma, M. Unno and A. Fujii for technical support, and H. Yamaguchi, M. Yoshioka and S. Kato for secretarial assistance. This work was supported by a Grant-in-Aid for Scientific Research from the Ministry of Education, Culture, Sports, Science and Technology of Japan (JSPS KAKENHI Grant numbers 24790489 for T.I. and 24229004 for T.S.).

Authors contributions

T.I. designed and performed the experiments and wrote the paper; C.I., M.E.S.G.B., Y.K., A.H-T. and H.H performed the experiments; T.K., O.T., K.J.I., S.T., T.N., F.B., G.N.B. and S.A. provided knockout mice; T.S. designed the experiments and wrote the paper.

Additional information

Supplementary Information accompanies this paper at http://www.nature.com/naturecommunications

Competing financial interests: The authors declare no competing financial interests.

Reprints and permission information is available online at http://npg.nature.com/reprintsandpermissions/

How to cite this article: Imanishi, T. *et al.* Nucleic acid sensing by T cells initiates Th2 cell differentiation. *Nat. Commun.* 5:3566 doi: 10.1038/ncomms4566 (2014).

© 2014 Macmillan Publishers Limited. All rights reserved.

RESEARCH ARTICLE SUMMARY

MUCOSAL IMMUNOLOGY

Innate lymphoid cells regulate intestinal epithelial cell glycosylation

Yoshiyuki Goto, Takashi Obata, Jun Kunisawa, Shintaro Sato, Ivaylo I. Ivanov, Aayam Lamichhane, Natsumi Takeyama, Mariko Kamioka, Mitsuo Sakamoto, Takahiro Matsuki, Hiromi Setoyama, Akemi Imaoka, Satoshi Uematsu, Shizuo Akira, Steven E. Domino, Paulina Kulig, Burkhard Becher, Jean-Christophe Renauld, Chihiro Sasakawa, Yoshinori Umesaki, Yoshimi Benno, Hiroshi Kiyono*

INTRODUCTION: The combination of food intake and the resident gut microbiota exposes the gastrointestinal (GI) tract to numerous antigens. Intestinal epithelial cells (ECs) compose a physical barrier separating the internal organs from the gut microbiota and other pathogenic microorganisms entering the GI tract. Although anatomically contained, the gut microbiota is essential for developing appropriate host immunity. Thus, the mucosal immune system must simultaneously maintain homeostasis with the gut microbiota and protect against infection by pathogens. Maintenance of the gut microbiota requires epithelial cell-surface glycosylation, with fucose residues in particular. Epithelial fucosylation is mediated by the enzyme fucosyltransferase 2 (Fut2). Polymorphisms in the *FUT2* gene are associated with the onset of multiple infectious and inflammatory diseases and metabolic syndrome in humans.

RATIONALE: Despite its importance, the mechanisms underlying epithelial fucosylation in the GI tract is not well understood. In particular, although commensals such as *Bacteroides thetaiotaomicron* induce epithelial fucosylation, how mucosal immune cells participate in this process is unknown. We used a combination of bacteriological, gnotobiological, and immunological techniques to elucidate the cellular and molecular basis of epithelial fucosylation by mucosal immune cells in mice, especially innate lymphoid cells (ILCs). To explore the role of ILCs in the induction and maintenance of epithelial fucosylation, we used genetically engineered mice lacking genes associated with the development and function of ILCs. To investigate the physiological functions of ILC-induced epithelial fucosylation, we used a Fut2-deficient mouse model of *S. typhimurium* infection.

ON OUR WEB SITE

Read the full article at http://dx.doi.org/10.1126/science.1254009

RESULTS: The induction and maintenance of Fut2 expression and subsequent epithelial fucosylation in the GI tract required type 3 ILCs (ILC3s) that express the transcription factor RORγt and the cytokines interleukin-22 (IL-22) and lymphotoxin (LT). Commensal bacteria, including segmented filamentous bacteria (SFB), induced fucosylation of intestinal columnar ECs and goblet cells. Expression of IL-22 by ILC3 required commensal bacteria, whereas LT was expressed in a commensal-independent manner. Ablation of IL-22 or LT in ILC3 resulted in a marked reduction in epithelial fucosylation, demonstrating that both cytokines are critical for the induction and regulation of epithelial fucosylation. Fucosylation of ECs in response to the intestinal pathogen *S. typhimurium* was also mediated by ILC3. Compared with control mice, Fut2-deficient mice were more susceptible to pathogenic inflammation as a result of *S. typhimurium* infection, suggesting that epithelial fucosylation contributes to host defense against *S. typhimurium* infection.

CONCLUSION: We demonstrate the critical role of the cytokines IL-22– and/or LT-producing ILC3 in the induction and regulation of intestinal epithelial fucosylation. We also show that ILC3-mediated epithelial fucosylation protects the host from invasion of *S. typhimurium* into the intestine. Our results provide important details of the glycosylation system and homeostatic responses created by the trilateral ILC3–EC–commensal axis in the intestine. Modulation of mucosal immune cell–mediated epithelial glycosylation may provide novel targets for the treatment or prevention of infectious diseases in humans. ■

RELATED ITEMS IN *SCIENCE*

L. V. Hooper, Innate lymphoid cells sweeten the pot. *Science* **345**, 1248–1249 (2014).

The list of author affiliations is available in the full article online.
*Corresponding author. E-mail: kiyono@ims.u-tokyo.ac.jp
Cite this article as: Y. Goto *et al.*, *Science* **345**, 1254009 (2014). DOI: 10.1126/science.1254009

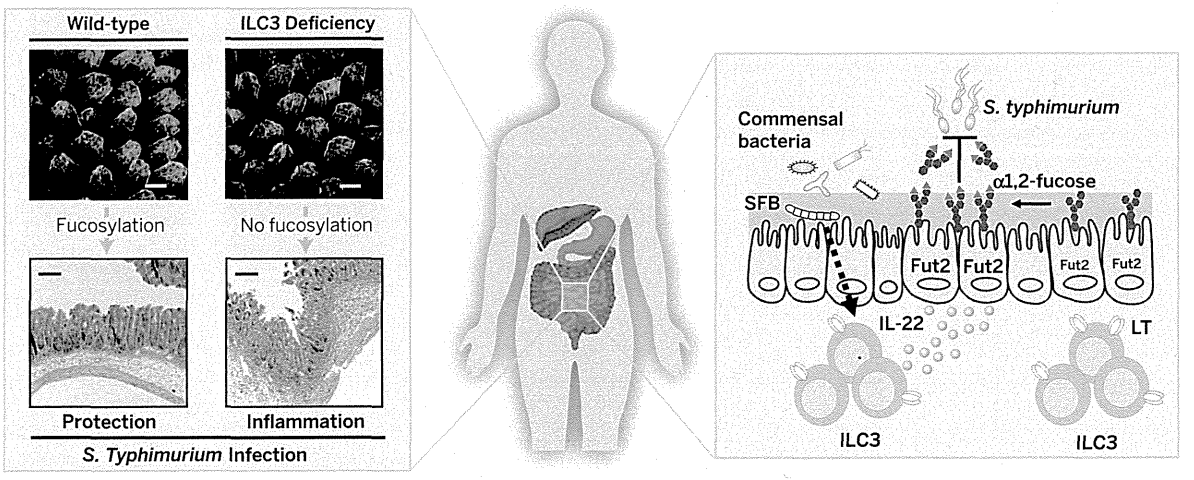

ILC3s regulate epithelial glycosylation. Commensal bacteria, including segmented filamentous bacteria (SFB), induce IL-22 production by ILC3. LT is produced by ILC3 in a commensal bacteria–independent manner. ILC3-derived IL-22 and LT cooperatively induce the production of Fut2 and subsequent epithelial fucosylation, which protects the host against *Salmonella typhimurium* infection.

Published by AAAS